NAL PROPOSAL No. 258

Scientific Spokesman:

P. A. Piroué
Department of Physics
Joseph Henry Laboratories
Princeton University
Princeton, New Jersey 08540

FTS/off-net: 8 (609) 599-3511
452-3000

A PROPOSAL TO MEASURE PARTICLES PRODUCED AT HIGH TRANSVERSE MOMENTUM BY PIONS

J. W. Cronin, H. J. Frisch, and M. J. Shochet
The Enrico Fermi Institute, University of Chicago
Chicago, Illinois 60637

and

J. P. Boymond, P. A. Piroué, and R. L. Sumner
Department of Physics, Joseph Henry Laboratories
Princeton University, Princeton, New Jersey 08540

October 1973

A PROPOSAL TO MEASURE PARTICLES PRODUCED AT HIGH TRANSVERSE MOMENTUM BY PIONS

J. W. Cronin, H. J. Frisch, and M. J. Shochet
The Enrico Fermi Institute, University of Chicago,
Chicago, Illinois, 60637

and

J. P. Boymond, P. A. Piroué*, and R. L. Sumner
Department of Physics, Joseph Henry Laboratories
Princeton University, Princeton, New Jersey 08540

Abstract

We propose to measure single particle inclusive spectra at high transverse momenta for incident pions. A coarse negative pion beam with 10^{10} particles/pulse and $\Delta p/p \sim 0.1$ is proposed. We wish to compare the pion induced spectra with proton induced spectra already measured in E-100. The pion intensity is sufficient to obtain inclusive spectra up to a transverse momentum of $\sim$6 GeV/c.

*Correspondent

Introduction

We propose to use the E-100 spectrometer to measure the yields of particles produced at high transverse momenta by negative pions incident on a heavy target (and possibly a H_2 target). A simple arrangement with a quadrupole triplet and a bending magnet can produce a pion beam of $\sim 10^{10}$ π^- / 10^{13} interacting protons at half the incident proton energy.

Our physics motivation is to study the production of particles at high transverse momenta with incident pions in place of protons. If there is any truth to the notion that quarks or partons play an important role in high $p_\perp$ phenomena, it would seem that replacing incident protons by pions should lead to significant differences in the ratios of the secondary particles produced. Also direct muon production might be enhanced because of the definite anti-quark content of a pion beam.

Pion Beam

We propose to make a pion beam similar to the one described in the attached Aspen Summer Study Report (Attachment 1). We have now made exact computer calculations and find that the conclusions of the report are substantially correct. The arrangement for the pion beam is shown in Fig. 1.

Fig. 2 shows the efficiency for collection of the pions as a function of $\Delta p/p$ measured with respect to the nominal momentum of the beam. A substantial fraction of all pions produced in the neighborhood of the selected momentum strike a 0.2 in. high by 0.6 in. wide target. Using the total integrated π^- yields from Fig. 3 of Attachment 1, we find a yield of 1.0×10^{-3} π^- at 200 GeV per interacting proton at 400 GeV.

The magnification of the E100 spectrometer converts the 0.2" x 0.6" target into an image 3.5" high and 1.8" wide at the final hodoscope. By enlarging the final hodoscope from its present dimension (3 in. x 6 in.) to a height of 5 in. and width of 7 in. we can preserve the acceptance of the spectrometer at its present value of $\Delta\Omega\Delta p/p = 1.7 \times 10^{-6}$.

As shown in Fig. 1, the vertical deflection of the beam allows additional apparatus to be placed symmetrically on the opposite side of the beam. By reversal of the magnet polarities, a positive beam can be placed on the target. If the selected energy is > 0.8 of the incident proton energy, the secondary beam is almost pure protons, and a comparison of the yields from protons and pions can be made. Knowledge of the relative pion and proton yields (as given for example in Fig. 1 of Attachment 1) permits the determination of the relative pion and proton cross sections. The determination of the absolute pion flux by radio chemical means may also be possible.

Rates

Attachment 2 is a copy of a paper recently submitted to Physical Review Letters. In this paper we present the results of high transverse momentum particle production by protons. The average intensity for these runs was $\sim 10^{11}$ protons/pulse and the duration of the actual running time consumed was less than three calendar months. Under these conditions we were able to obtain the data presented in Attachment 2, which reach a transverse momentum of 7.5 GeV/c.

In Table I we give the maximum transverse momentum we can expect to reach in a similar period of time with pions. These limits are based

on the assumption that the pion induced cross sections are the same as the proton induced cross sections. The limits are given for two operating conditions of the N.A.L. machine. The first, 3×10^{12} protons/pulse at 300 GeV, is within the present machine capability. The second, 2×10^{13} protons/pulse at 400 GeV, is what we hope would be available when this experiment is in operation. One should note that the high intensity is required only for the points above $p_\perp = 3$ GeV/c. At lower $p_\perp$ the data taking rate is limited by factors other than intensity.

The limit on $p_\perp$ does not appear to be a sensitive function of the pion momentum. This is because the decreasing pion flux is compensated by the rising cross section. The particle ratios can be measured with reasonable precision up to a $p_\perp \sim 1$ GeV/c less than the maximum obtainable $p_\perp$ given in Table I.

Location of the Experiment

The proposed pion beam requires $\sim$ 200' between the production target and the pion focus. The final proton dump can be about 10' down stream from the pion target. It would be possible to install this arrangement in the P-Central laboratory after the completion of the present experiment there. One could use the present target box for the pion production target. At the downstream end of P-Central one could install a second target box containing the target struck by the pions and the final proton dump. Additional space behind is available for the 250' long excavation that would be required for the relocation of the E-100 spectrometer.

We mention this scheme to suggest that a feasible arrangement might be developed without major new construction. The construction suggested here is in the original spirit of the flexible Proton Laboratory concept.

Time Scale

Since the E-100 apparatus exists and requires only small modifications, the experiment could begin as soon as the pion beam could be prepared.

TABLE I

Maximum Observable Transverse Momentum (GeV/c)

Pion Energy	300 GeV 3×10^{12} protons/pulse	400 GeV 2×10^{13} protons/pulse
100	5.5	6.2
150	5.5	6.2
200	5.3	6.2
250	∿5.0	6.2
300	-	6.2
350	-	∿5.4

FIGURE CAPTIONS

Fig. 1. Schematic arrangement of pion beam.
Note difference in horizontal and vertical scales.

Fig. 2. Collection efficiency for $\sim$ 200 GeV pions as a function of $\Delta p/p$ measured with respect to the central momentum.

TABLE CAPTION

The value of the maximum observable transverse momentum is given as a function of pion energy for the two indicated machine operating conditions.

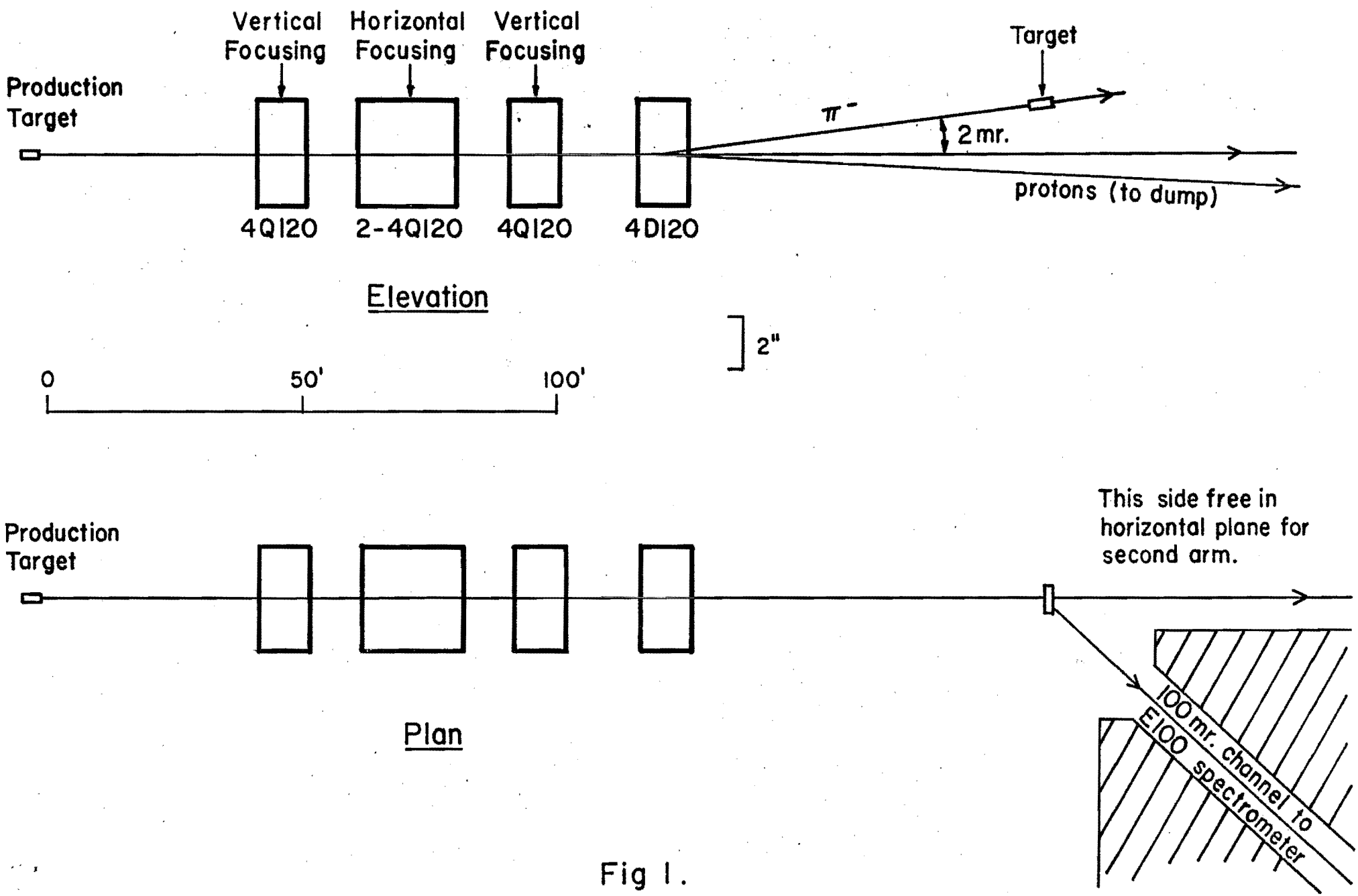
Vertical Focusing
Horizontal Focusing
Vertical Focusing
Production Target
Target
π^-
2 mr.
protons (to dump)
4Q120
2-4Q120
4Q120
4D120
Elevation
2"
0
50'
100'
Production Target
This side free in horizontal plane for second arm.
100 mr. channel to E100 spectrometer
Plan

Fig 1.

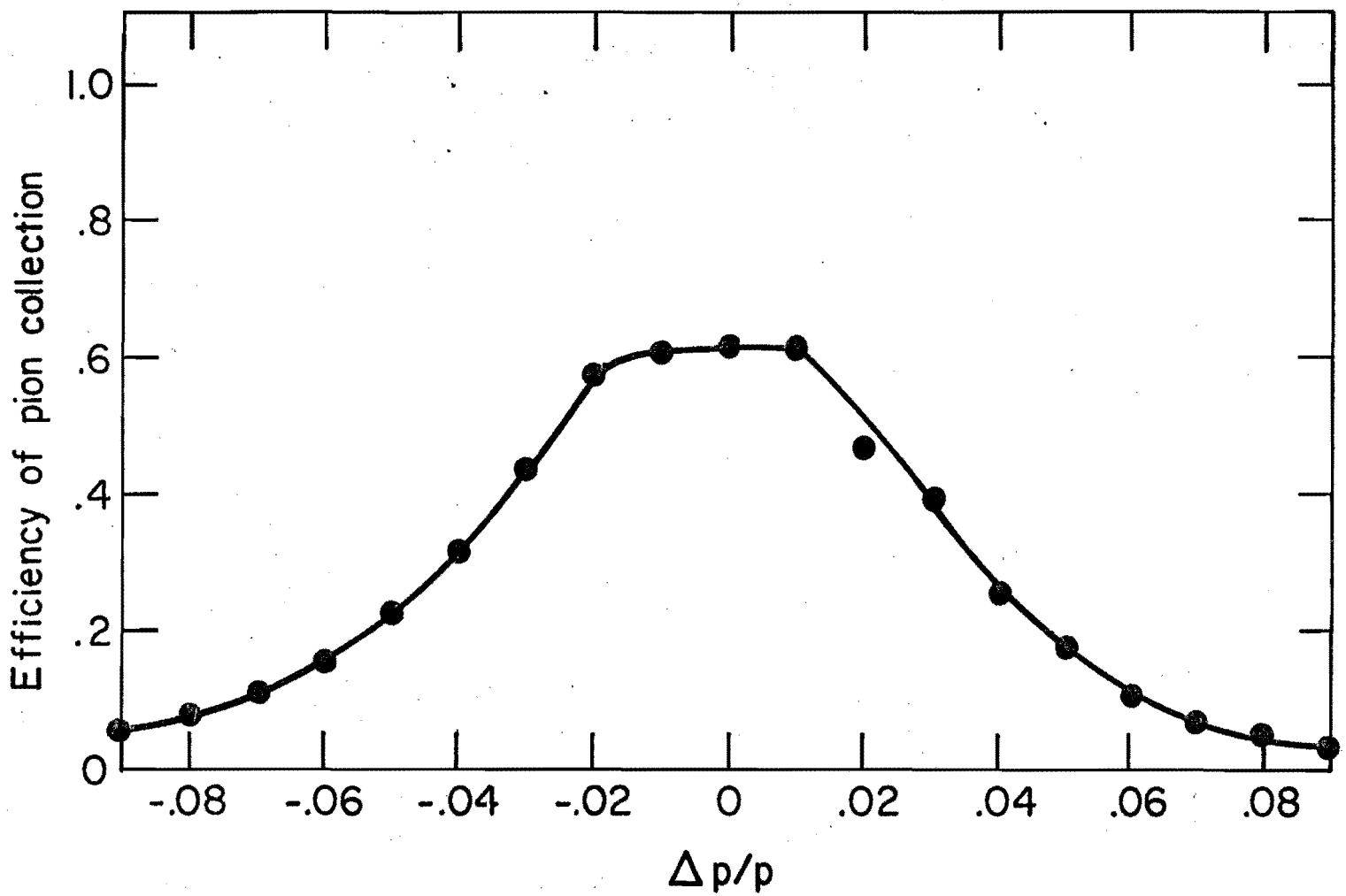
Efficiency of pion collection
1.0
.8
.6
.4
.2
0
-.08
-.06
-.04
-.02
0
.02
.04
.06
.08
Δp/p

Fig 2.

Attachment 1

A "SPECIAL" HIGH INTENSITY PION BEAM

(NAL Summer Study, July 30, 1973)

J. W. Cronin
Enrico Fermi Institute, University of Chicago

I. Introduction

We discuss here a "special" high intensity pion beam which is based on the following design criteria.

1) The highest intensity possible
2) Large $\Delta p/p$
3) Spot size $\sim$ 1/4" x 1/4"
4) The spatial definition of the pion beam can be determined by size of the target.

Based on these criteria we suggest a possible beam arrangement. This beam is suitable for the study of particle production at high transverse momenta. It is also suitable for the production of pion induced tertiary beams such as a K_0 beam which would be relatively free of neutrons. This beam would not be suitable for more traditional applications such as total cross sections, elastic scattering, small angle inclusive studies, etc.

II. Yields

We have used the formulae of C. L. Wang (BNL, CRISP Report 72-69) for the invariant pion production cross sections. These fit all existing data from the AGS, CERN, and ISR within a factor 2 and explicitly make use of scaling. Figure 1 shows the invariant cross section $E\frac{d^3\sigma}{dp^3}$ for π^+ and π^- production at $p_\perp = 0$. The proton cross

sections were obtained from the report of Sens at the Batavia Conference.

Figures 2 and 3 show the possible yields of π^+ and π^- mesons respectively for large solid angle, 12 μster and 3 μster. The natural collimation of pions is clear from the fact that a major fraction of all the pions produced are collected with a 12 μster solid angle.

For a positive pion beam the contamination of protons will be one to one at 80 GeV and greater than 10 to 1 for energies greater than 220 GeV. This contamination is too large for the positive beam to be used for the purposes stated above, namely particle production by pions, and neutron free K_0 beams. Therefore we concentrate on a negative pion beam.

III. Proposed Beam

Figure 4 shows the proposed idea for the beam. The quadrupole triplet focuses the pions from the production onto a secondary target. For 200 GeV the gradients required are ∿6 Kg/in. Since the beam is designed only for negative pions a very small dispersion is required to separate the negative pions from the primary protons. The nominal deflection of the pions is 1.8" at 75'. When using the beam for pions from 100 GeV to 300 GeV the proton beam is deflected by 0.45" and 1.35" respectively in the opposite direction. The triplet lense also tends to refocus the primary beam. If the emittance of the primary beam is less than 0.5 mm.-mrad, then there should be no difficulty with the tails of the primary beam striking the secondary target.

The size of the secondary spot is dominated by chromatic abberation of the lens due to the large momentum spread of the desired pion beam. Figure 5 shows the projected spot sizes at the position of the secondary target due to chromatic abberation. Superimposed on this should be a size $\sim$.08" diameter (2mm.) due to a 1 mm diameter primary spot. We neglect this size in the foregoing calculations. Figure 6 shows the approximate solid angle vs $\Delta p/p$ for the proposed beam, for targets of .2" V x .3" H and .1" V x .2"H. At 200 GeV/c one would have yields of 1.9×10^{-3} π^- proton and 1.1×10^{-3} π^-/proton respectively.

IV. Physics

Our physics motivation is to study the production of particles at high transverse momentum with pions replacing protons. If there is any sense to the notion of quarks or partons it would seem that replacing incident protons by pions should lead to significant differences in the ratios of secondary particles produced and the cross sections for their production. Also direct muon production might be enhanced because of the definite anti parton content of a pion beam. Figure 7 shows some preliminary data obtained with protons striking a 1/8" diameter tungsten target. The mean intensity was 1.5×10^{11} protons/pulse and the counting rate at 7.5 GeV/c was $\sim$5 counts/hour. With a pion beam $\sim 10^{10}$/pulse we might expect to reach the same sensitivity with runs of 10 hours.

V. Where to Install?

There are many possibilities. The pion beam is 200' long and the spectrometer that follows is 300', so 500' of linear space is required. If one neglects interference with ongoing programs such a beam could be fitted into the present P-Central lab with the requirement that 300' of new tunnel be built for the spectrometer at 80 mrad. A pion beam and 90^{0} CM spectrometer is very much in scale with many experiments and cannot be considered an extraordinary development.

VI. Acknowledgements

The author appreciates numerous discussions about pion beams with Bradley Cox. A conversation with Roy Rubenstein was particularly valuable in formulating the present proposal.

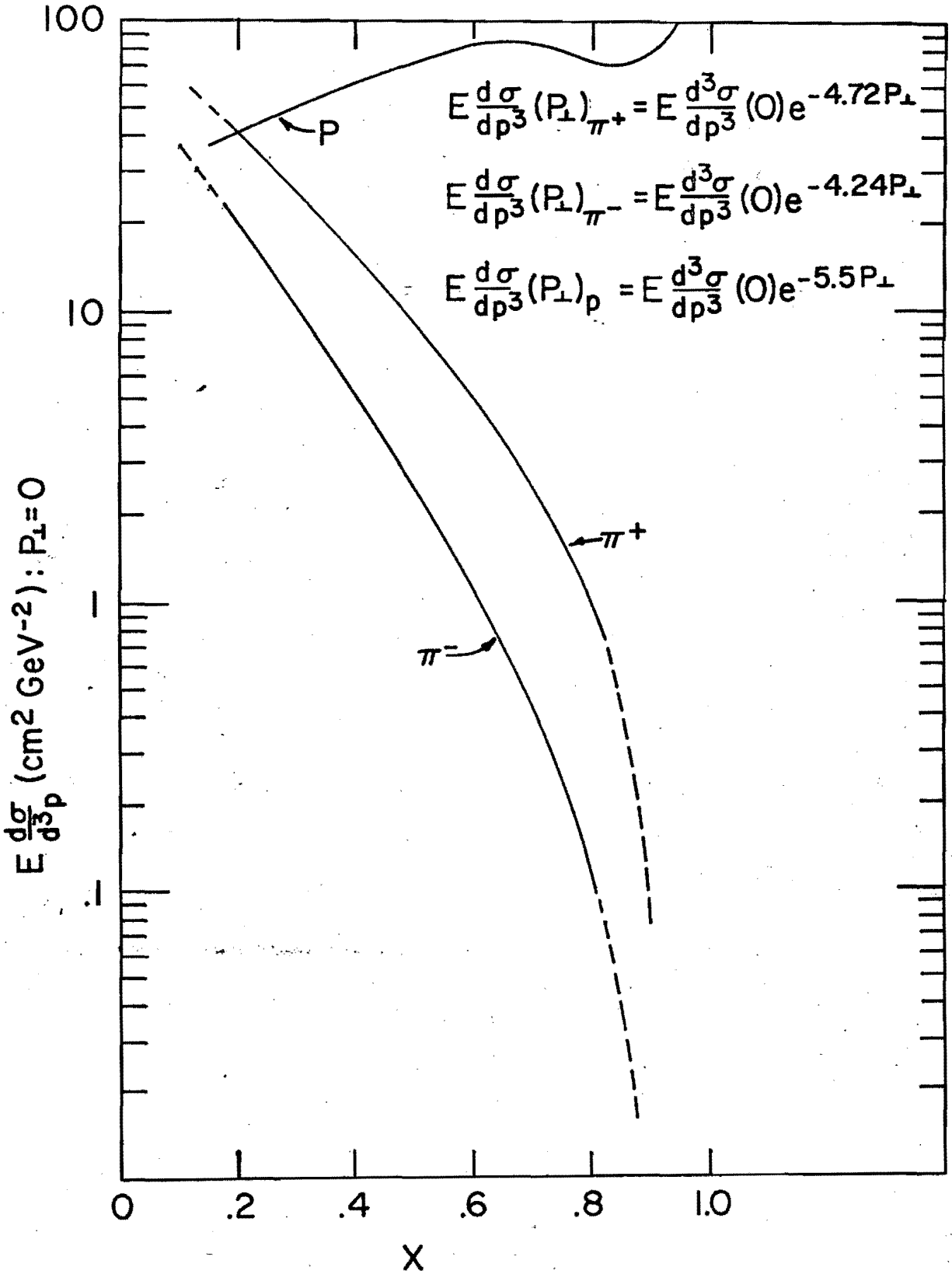
100
10
1
.1
0
.2
.4
.6
.8
1.0
X
$E\frac{d\sigma}{d^3p}$ (cm^2 GeV^{-2}) ; $P_\perp = 0$
$E\frac{d\sigma}{dp^3}(P_\perp)_{\pi^+} = E\frac{d^3\sigma}{dp^3}(0)e^{-4.72P_\perp}$
$E\frac{d\sigma}{dp^3}(P_\perp)_{\pi^-} = E\frac{d^3\sigma}{dp^3}(0)e^{-4.24P_\perp}$
$E\frac{d\sigma}{dp^3}(P_\perp)_{p} = E\frac{d^3\sigma}{dp^3}(0)e^{-5.5P_\perp}$
P
π^+
π^-

Fig 1.

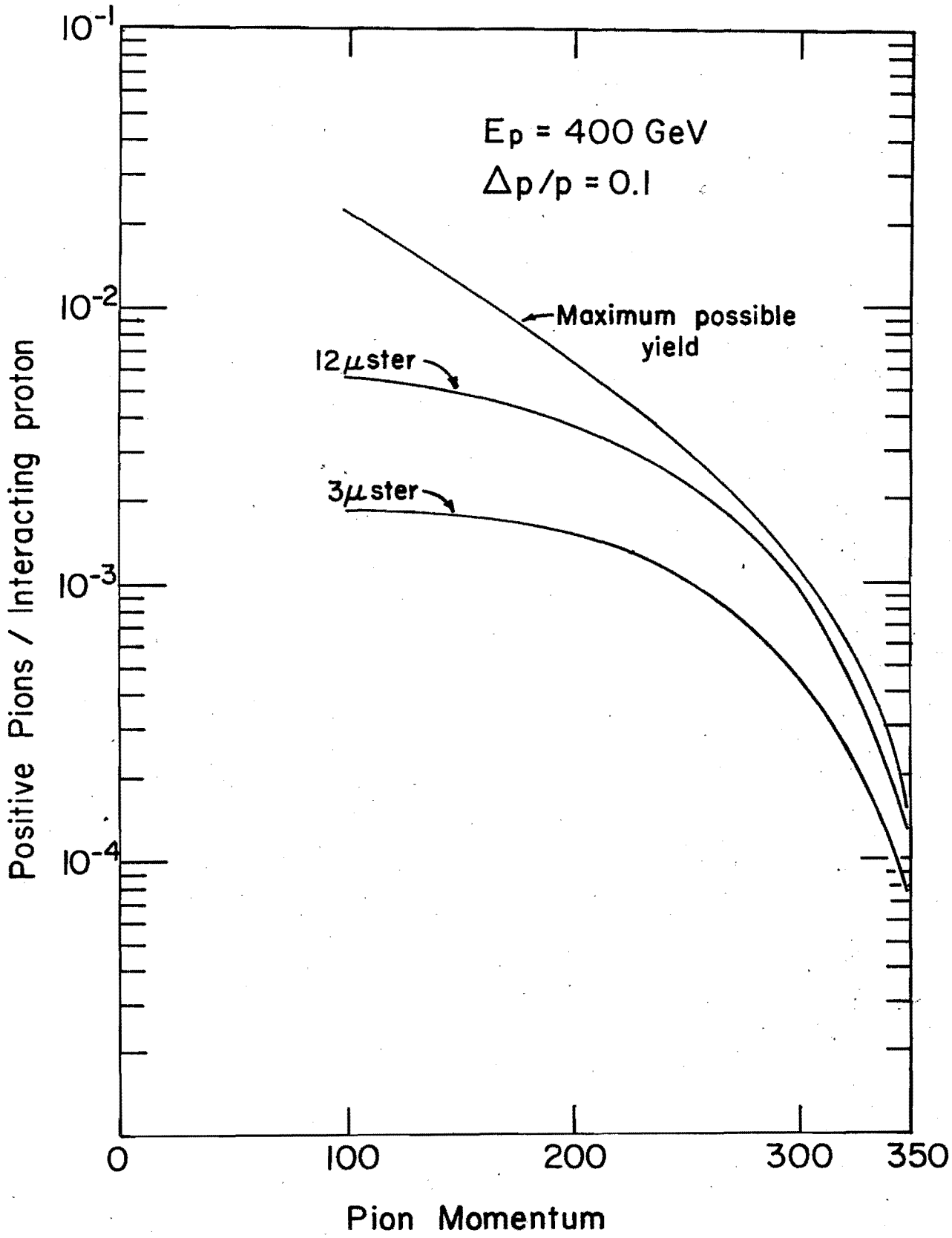
10^{-1}
10^{-2}
10^{-3}
10^{-4}
E_p = 400 GeV
$\Delta p/p$ = 0.1
Maximum possible yield
12 μster
3 μster
Positive Pions / Interacting proton
0
100
200
300
350
Pion Momentum

Fig 2.

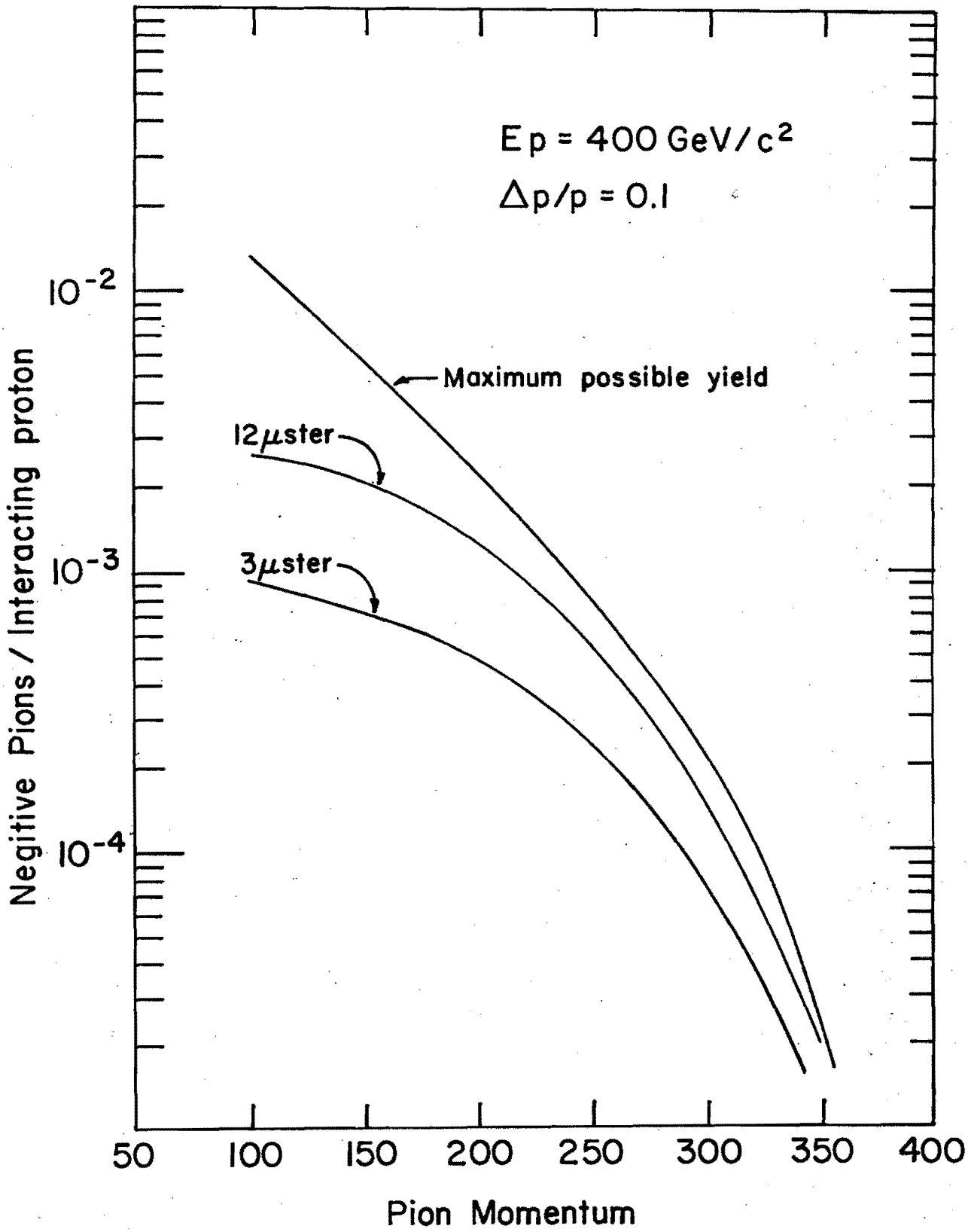
Ep = 400 GeV/c²
Δp/p = 0.1
Maximum possible yield
12μster
3μster
10⁻²
10⁻³
10⁻⁴
Negitive Pions / Interacting proton
50
100
150
200
250
300
350
400
Pion Momentum

Fig 3.

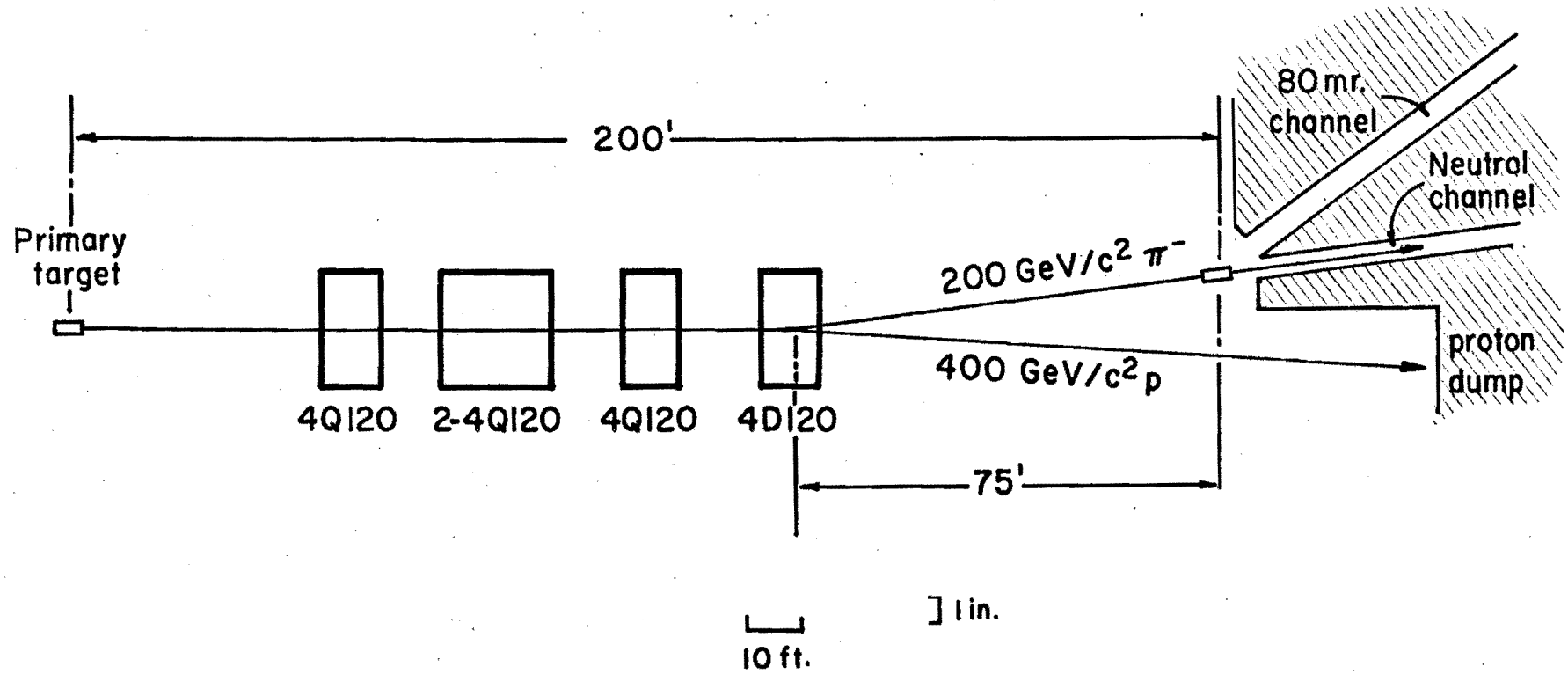
200'
Primary target
4Q120
2-4Q120
4Q120
4D120
200 GeV/c² π⁻
400 GeV/c² p
75'
80 mr. channel
Neutral channel
proton dump
10 ft.
1 in.

Fig 4.

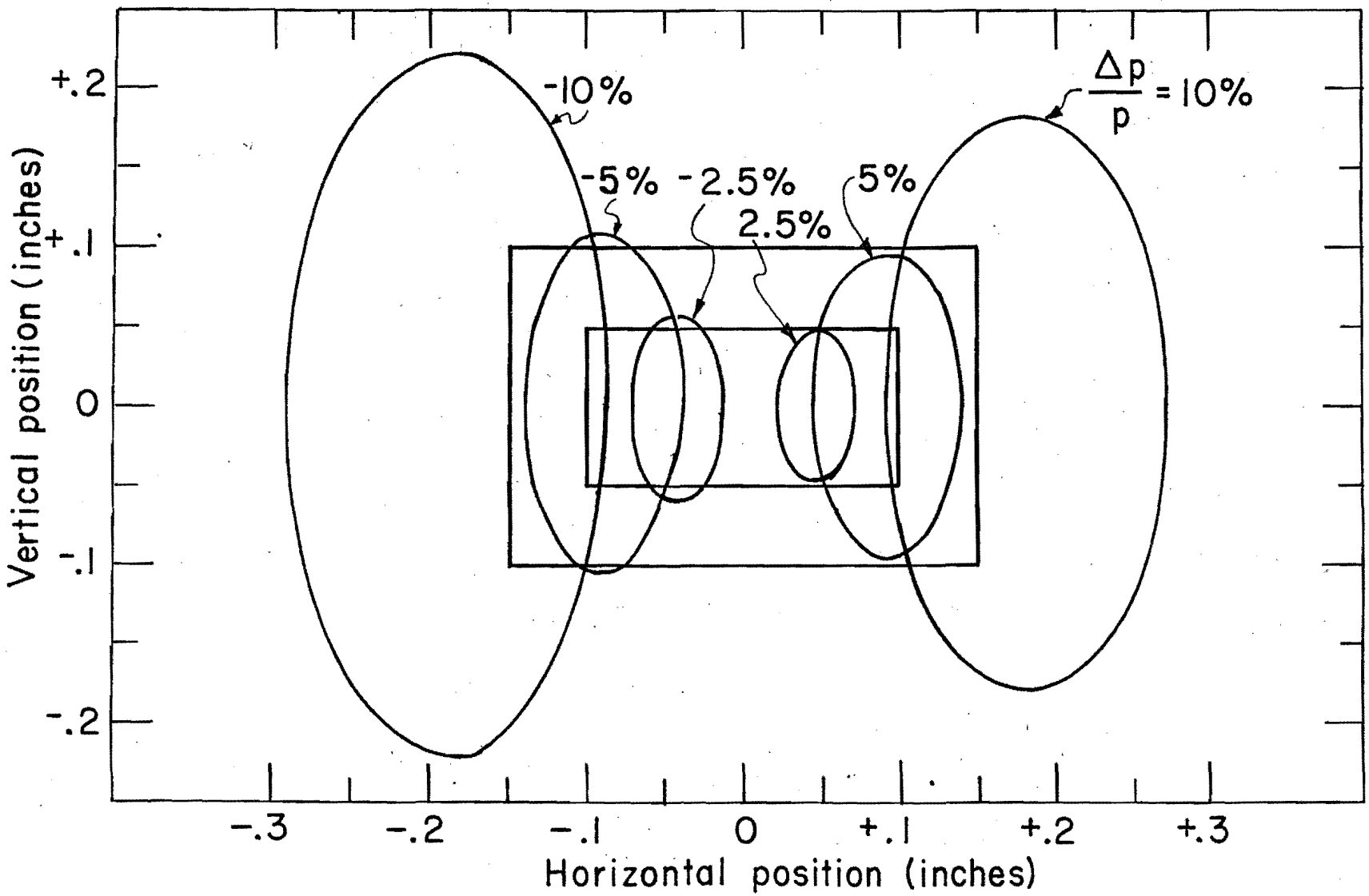
-10%
-5%
-2.5%
2.5%
5%
$\frac{\Delta p}{p} = 10\%$
+.2
+.1
0
-.1
-.2
Vertical position (inches)
-.3
-.2
-.1
0
+.1
+.2
+.3
Horizontal position (inches)

Fig 5.

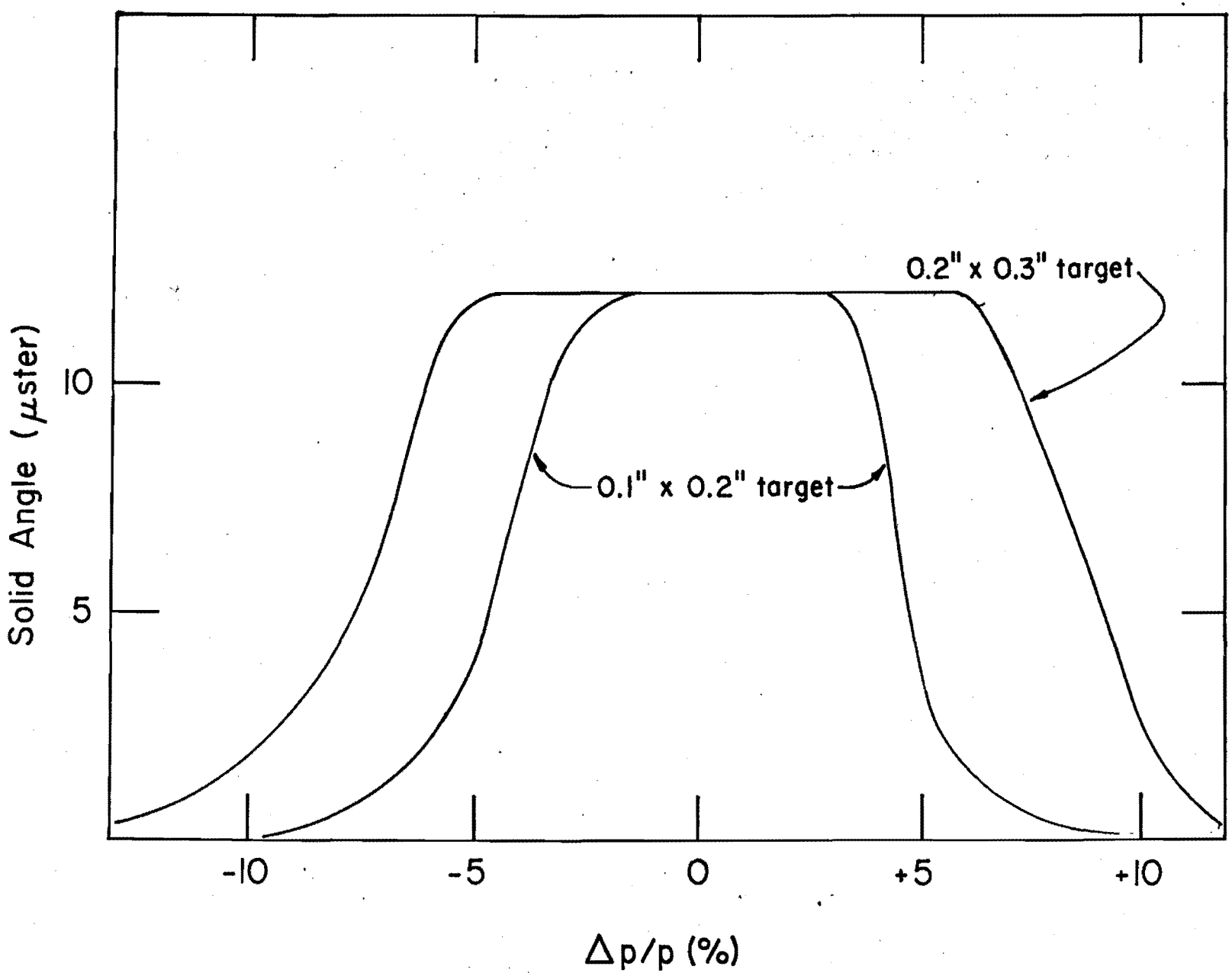
0.2" x 0.3" target
0.1" x 0.2" target
Solid Angle (μster)
10
5
-10
-5
0
+5
+10
Δp/p (%)

Fig 6.

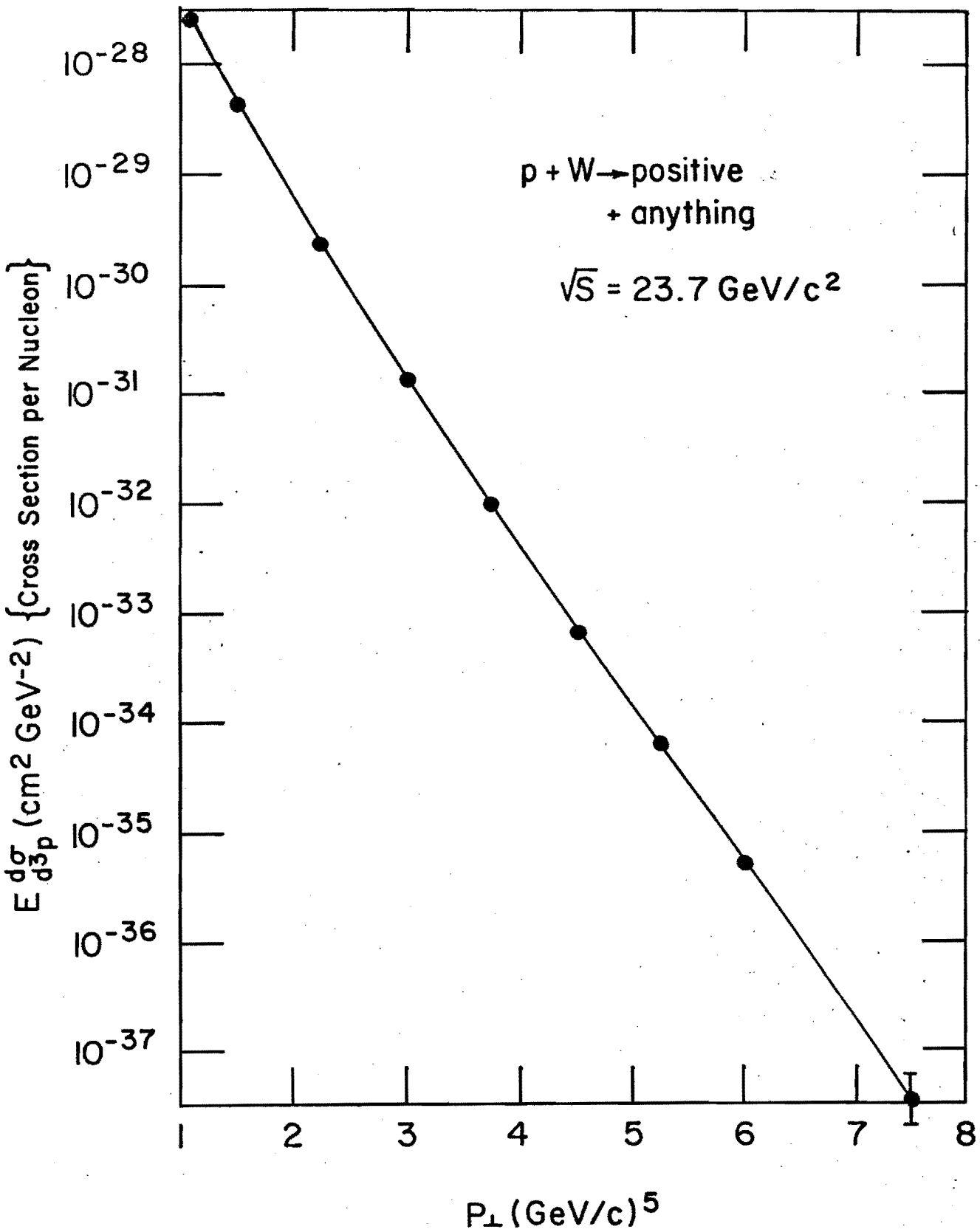
p + W → positive
+ anything
√S = 23.7 GeV/c²
10⁻²⁸
10⁻²⁹
10⁻³⁰
10⁻³¹
10⁻³²
10⁻³³
10⁻³⁴
10⁻³⁵
10⁻³⁶
10⁻³⁷
E dσ/d³p (cm² GeV⁻²) {Cross Section per Nucleon}
1
2
3
4
5
6
7
8
P⊥ (GeV/c)⁵

Fig 7.

Production of Hadrons with Large Transverse Momentum at 200 and 300 GeV*

J. W. Cronin, H. J. Frisch, and M. J. Shochet

The Enrico Fermi Institute, University of Chicago, Chicago, Illinois 60637

and

J. P. Boymond, P. A. Piroué, and R. L. Sumner

Department of Physics, Joseph Henry Laboratories

Princeton University, Princeton, New Jersey 08540

ABSTRACT

Differential cross sections as a function of transverse momentum are presented for the production at $\sim 90^{\circ}$ c.m. of $\pi^{\pm}$, $K^{\pm}$, p, and $\bar{p}$ in p-nucleus collisions at incident proton energies of 200 and 300 GeV.

Investigations of large transverse momentum ($p_{\perp}$) phenomena are interesting because of their possible relation to basic processes at small distances. Experimentally, it had been known[1] for some time that the $p_{\perp}$ distributions of long-lived particles produced in high-energy hadron collisions were falling off exponentially ($e^{-bp_{\perp}}$), with the average transverse momentum $\langle p_{\perp} \rangle = 0.3 - 0.5$ GeV/c, independent both of the secondary particle energy E and of the c.m. energy $\sqrt{s}$ of the collision. Recent measurements[2] at the CERN Intersecting Storage Rings (ISR) have in general confirmed these $\langle p_{\perp} \rangle$ values. However, at high $p_{\perp}$ (> 3 GeV/c), a much more copious pion production has been observed[3,4,5] than predicted by the extrapolation of the data at small $p_{\perp}$ (< 1 GeV/c).

In an experiment at the National Accelerator Laboratory (NAL) we have measured, as a function of $p_\perp$, the invariant cross section $Ed\sigma/d^3p$ for the production of $\pi^\pm$, $K^\pm$, p, and $\bar{p}$ in p-nucleus collisions at incident proton energies of 200 and 300 GeV. The measurements were made in the region of 90° in the c.m. system of the incident proton and a single nucleon at rest.

Figure 1 shows a schematic view of the apparatus. The NAL proton beam, extracted from the main ring and transported ∿1.1 miles away to the target box of the Proton East Laboratory, impinged on a 2-in.-long, 1/8-in.-diam tungsten target. Particles emitted at 77 mrad ($\sim 90^\circ$ in the proton-nucleon c.m.) relative to the direction of the incident proton beam traversed a ∿330 ft.-long magnetic spectrometer consisting of a quadrupole doublet, 2 collimators, 2 bending magnets, and 4 scintillation hodoscopes H_1 - H_4. The momentum acceptance was 10% with a solid angle $\Delta\Omega$ = 17 μsr. Each hodoscope consisted of a 4-in.-wide, 2-in.-high, 1/4-in.-thick trigger counter (A) followed by an array of 5 horizontal and 17 vertical 1/8-in.-thick scintillator channels. This arrangement allowed us to determine the momentum of individual events to within ±1%, and to reconstruct the position of each track at the target to within ±0.4 in. horizontally, and ±0.08 in. vertically. This check was essential at high momentum to eliminate background.

Particles were identified in the Cerenkov counter located between H_3 and H_4. It was a 80-ft.-long, 1-ft.-diam stainless steel tube with non-reflecting walls, bolted to a 6-ft.-long, 2-ft.-diam optical section in which the Cerenkov light was split into 2 channels (0 - 9 and 9 - 38 mrad), and focussed on 2-in. photomultipliers (RCA 31000 M). Depending on the momentum and the particle type the counter was filled either with He or CO_2 at pressures ranging from ∿0 to 10 atm.

A charged particle was signalled by the coincidence $A_1A_2A_3A_4$. Information from the counters was fed to a PDP-9 computer. The hodoscope information was used to reconstruct particle tracks through the spectrometer back to the target.

The proton beam striking the target was monitored by 2 three-counter telescopes located at 90° relative to the direction of the incident proton beam and directed at the target. The absolute calibration of the monitors against the proton beam intensity was done in two ways (radiochemical and ion chamber). However, while the relative accuracy of the monitors was better than 5% their absolute calibration was estimated to be known only to ∿50%.

We measured the particle yields at laboratory momenta ranging from 10 to 100 GeV/c, corresponding to $p_\perp$ = 0.76 to 7.6 GeV/c. In order to handle the high counting rates encountered below 40 GeV/c smaller trigger counters were used and the hodoscopes removed. Accidental coincidences, monitored continuously, were found to be negligible except at high momenta (> 70 GeV/c) where the requirement that the observed events originated in the target was essential in the elimination of this background. The data were corrected for nuclear absorption and multiple Coulomb scattering in the apparatus (significant only below 20 GeV/c), and, when appropriate, for particle decay.

The particle yields were converted into equivalent cross sections in p-nucleon collisions by using the following formula:

$$Ed\sigma/d^3p = \sigma_p(\text{yield/incident proton})/p^2(\Delta\Omega\Delta p/p)f,$$

where p denotes the laboratory momentum, σ_p the proton-nucleon total cross section which we took to be 40 mb, and f is the fraction of incident protons interacting in the target. Using an absorption cross section in W of 1635 mb

one obtains, for a 2-in. target, f = 0.41. The quantity $\Delta\Omega\Delta p/p = 1.7 \times 10^{-6}$, the spectrometer acceptance, was calculated by Monte-Carlo techniques.

The production cross sections for $\pi^{\pm}$, and those for $K^{\pm}$, p, and $\bar{p}$ relative to pions of the same charge, are listed as a function of $p_{\perp}$, in Table I. In Fig. 2 we have plotted, as an illustration, the π^- cross section against $p_{\perp}$ at both incident proton energies. (The π^+ cross section has similar behavior.) We observe a fall-off with $p_{\perp}$ which is slower than exponential, and an energy dependence which, though very small at low $p_{\perp}$, becomes stronger as $p_{\perp}$ increases. This is in qualitative agreement with the work of the Saclay-Strasbourg group[3], and of the CERN-Columbia-Rockefeller group[4] at the ISR.

Most of the theoretical models[6] which have been proposed predict for the single pion inclusive cross section at $\sim 90^{\circ}$ c.m. a behavior, at high $p_{\perp}$, of the form $g(s)f(x_{\perp})$, where g(s) is some function (generally a power law) of s, the square of the c.m. energy of the collision, and $f(x_{\perp})$ is a function of the scaling variable $x_{\perp} = 2p_{\perp}/\sqrt{s}$. If our pion data can indeed be expressed in such a form, then the logarithm of the cross section plotted against $x_{\perp}$ at both c.m. energies (19.4 and 23.8 GeV) should yield parallel curves, independent of the absolute calibration. Figure 3 shows that this is approximately so only at large $x_{\perp}$(> 0.4) where, for example, the form $s^{-5.4}\exp(-36x_{\perp})$ is found to give a good representation of our data. At low $x_{\perp}$(< 0.3), however, the curves become slowly steeper as $\sqrt{s}$ increases (the higher energy curves are the ISR π^{o} data[4]).

The $K^{\pm}$, p and $\bar{p}$ yields relative to pions are displayed as functions of $x_{\perp}$ in Fig. 4. With the exception of p/π^+ the ratios do not change dramatically with incident proton energy. In fact for $x_{\perp} > 0.4$ the ratios are, to a good approximation, independent of energy. For $p_{\perp} > 3.0$ GeV/c the ratios of heavy particles ($K^{\pm}$, p, $\bar{p}$) to pions do not increase with $p_{\perp}$ as sug-

gested by measurements at the ISR at lower $p_\perp$[5]. As $x_\perp$ is increased from 0.2 to 0.5 the ratios K^-/K^+ and $\bar{p}/p$ decrease by a factor of ~ 2 and ~ 4, respectively. This is a feature qualitatively similar to that found in hadron production at small $x_\perp$ and large $x = 2p_{/\!/}/\sqrt{s}$.

Finally it should be mentioned that auxiliary measurements made with beryllium and titanium targets established that none of the important features observed in tungsten were dependent on atomic number.

We wish to express our appreciation to the staffs of NAL and especially of the Proton Area who have contributed enormous time and effort to make this experiment possible. We are also indebted to K. Wright for the excellent performance of the Cerenkov counter.

REFERENCES

*Work supported by the National Science Foundation and the U.S. Atomic Energy Commission.

1. See, for example, G. Cocconi, Nuovo Cimento 57 A, 837 (1968).
2. A. Bertin et al., Phys. Letters 42 B, 493 (1972); M. Banner et al., Phys. Letters 41 B, 547 (1972).
3. M. Banner et al., Phys. Letters 44 B, 537 (1973).
4. F. W. Büsser et al., CERN preprint (10 August 1973), to be published in Phys. Letters.
5. B. Alper et al., Phys. Letters 44 B, 521 and 527 (1973).
6. See, for example, S. M. Berman, J. D. Bjorken, and J. B. Kogut, Phys. Rev. D4, 3388 (1971); R. Blankenbecler, S. J. Brodsky, and J. F. Gunion, Phys. Letters 42 B, 461 (1972); P. V. Landshoff and J. C. Polkinghorne, Phys. Letters 45 B, 361 (1973); S. D. Ellis and M. B. Kislinger, NAL preprint Pub-73/40/THY, to be published in Phys. Rev.

FIGURE CAPTIONS

Fig. 1. Experimental arrangement

Fig. 2. Transverse momentum distribution of π^- mesons produced at $\sim 90^0$ c.m. in p-W collisions at incident proton energies of 200 and 300 GeV.

Fig. 3. The average of the π^+ and π^- invariant cross sections versus $x_\perp = 2p_\perp/\sqrt{s}$ at various c.m. energies. The data at $\sqrt{s}$ = 23.5, 30.6 44.8, and 52.7 GeV are those of Ref. 4 and refer to π^o. The discrepency between the data at 23.8 and 23.5 GeV should not be considered significant.

Fig. 4. Particle abundance relative to pions versus $x_\perp$.

TABLE CAPTION

Table I. Invariant cross section per nucleon (see text) $Ed\sigma/d^3p$ (cm^2 GeV^{-2}) for $\pi^\pm$ mesons produced at $\sim 90^o$ c.m. in p-W collisions, and particle ratios at 200 GeV and 300 GeV incident proton energies. At each $p_\perp$ value the top line refers to π^+, K^+/π^+, p/π^+, respectively, and the bottom line to π^-, K^-/π^-, $\bar{p}/\pi^-$. Errors on the cross sections do not include the uncertainty in the absolute calibration.

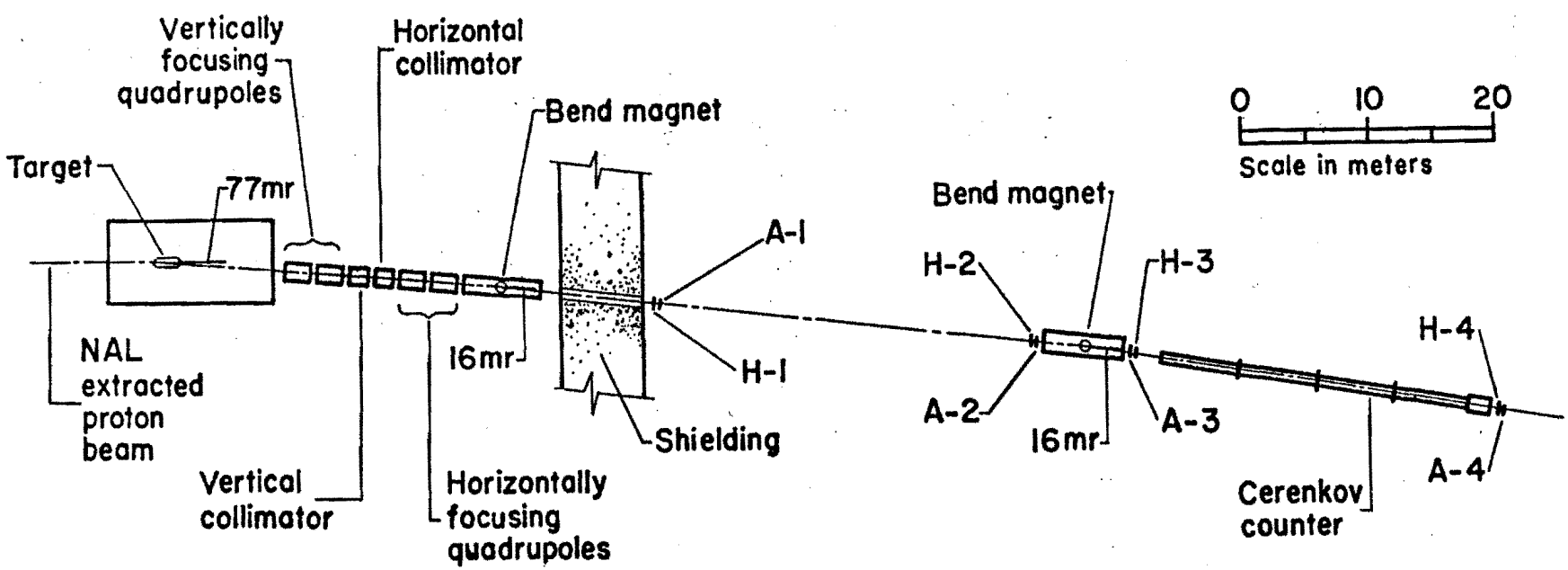
Vertically focusing quadrupoles
Horizontal collimator
Bend magnet
Target
77mr
A-1
H-1
16mr
Shielding
NAL extracted proton beam
Vertical collimator
Horizontally focusing quadrupoles
Bend magnet
H-2
H-3
A-2
16mr
A-3
H-4
A-4
Cerenkov counter
0
10
20
Scale in meters

Figure 1

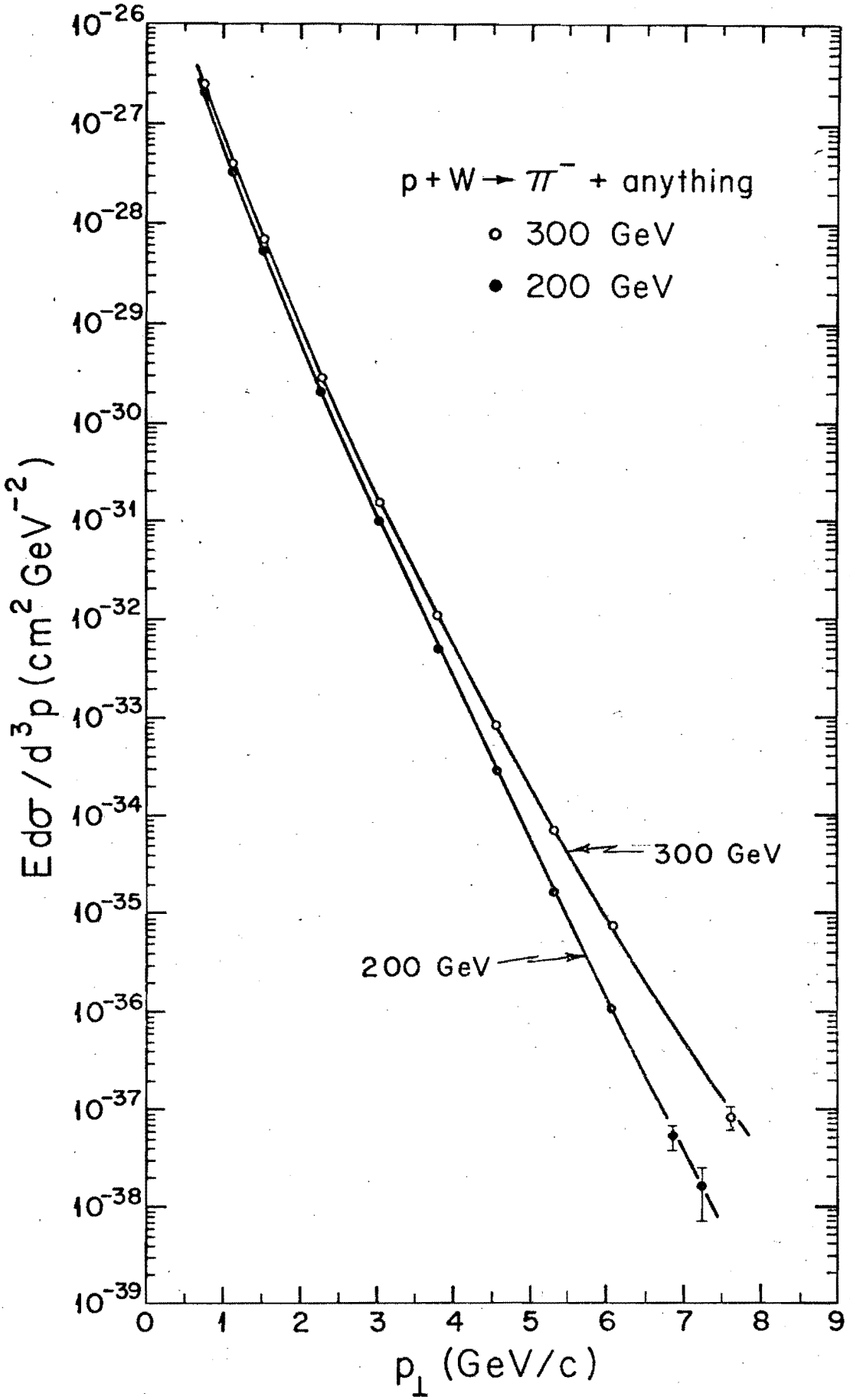
p + W → π⁻ + anything
300 GeV
200 GeV
300 GeV
200 GeV
E dσ / d³p (cm² GeV⁻²)
p⊥ (GeV/c)
10⁻²⁶
10⁻²⁷
10⁻²⁸
10⁻²⁹
10⁻³⁰
10⁻³¹
10⁻³²
10⁻³³
10⁻³⁴
10⁻³⁵
10⁻³⁶
10⁻³⁷
10⁻³⁸
10⁻³⁹
0
1
2
3
4
5
6
7
8
9

Figure 2

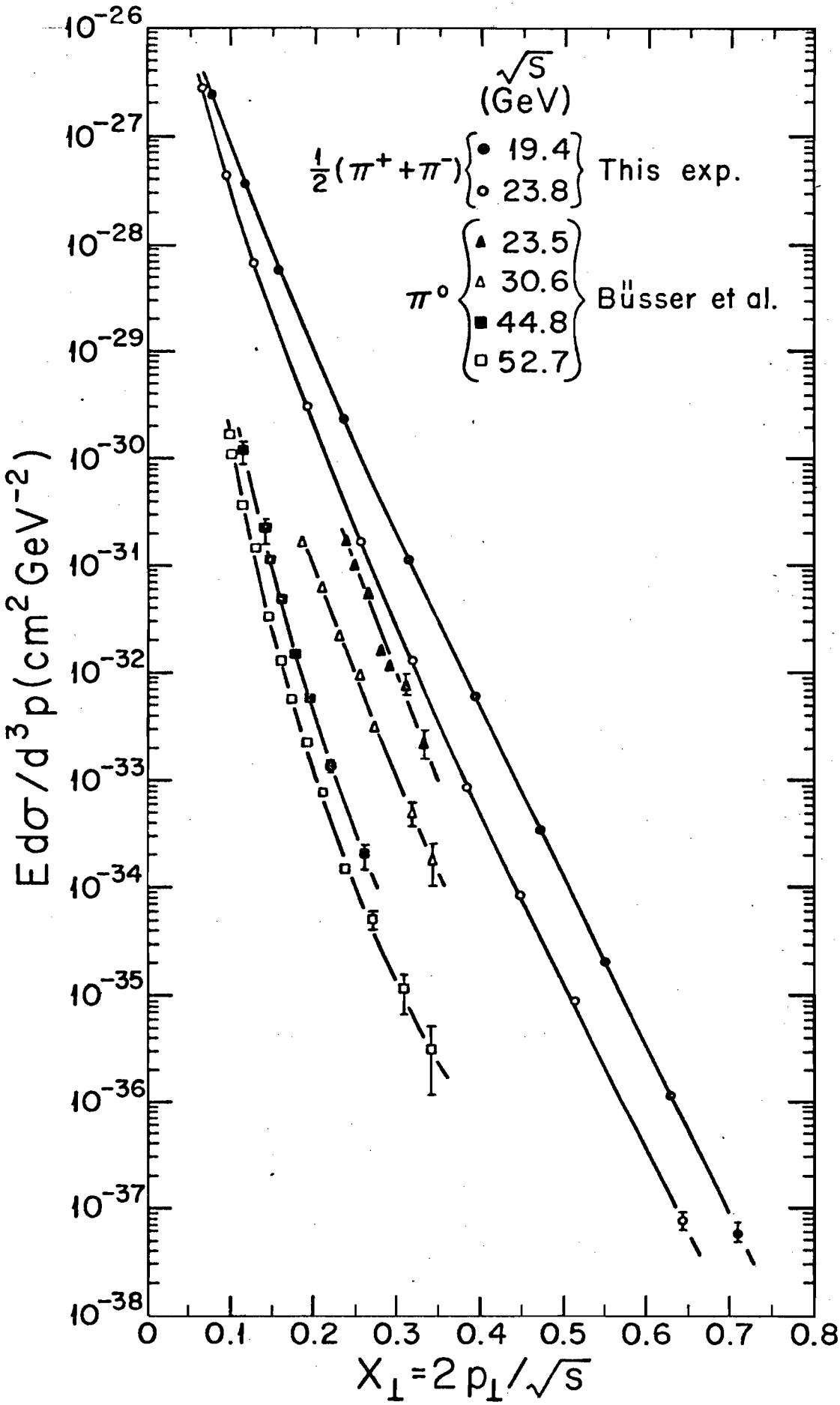
$\sqrt{S}$ (GeV)
$\frac{1}{2}(\pi^+ + \pi^-)$ 19.4 23.8 This exp.
π^0 23.5 30.6 44.8 52.7 Büsser et al.
$E d\sigma/d^3p\,(cm^2 GeV^{-2})$
$X_\perp = 2p_\perp/\sqrt{s}$

Figure 3

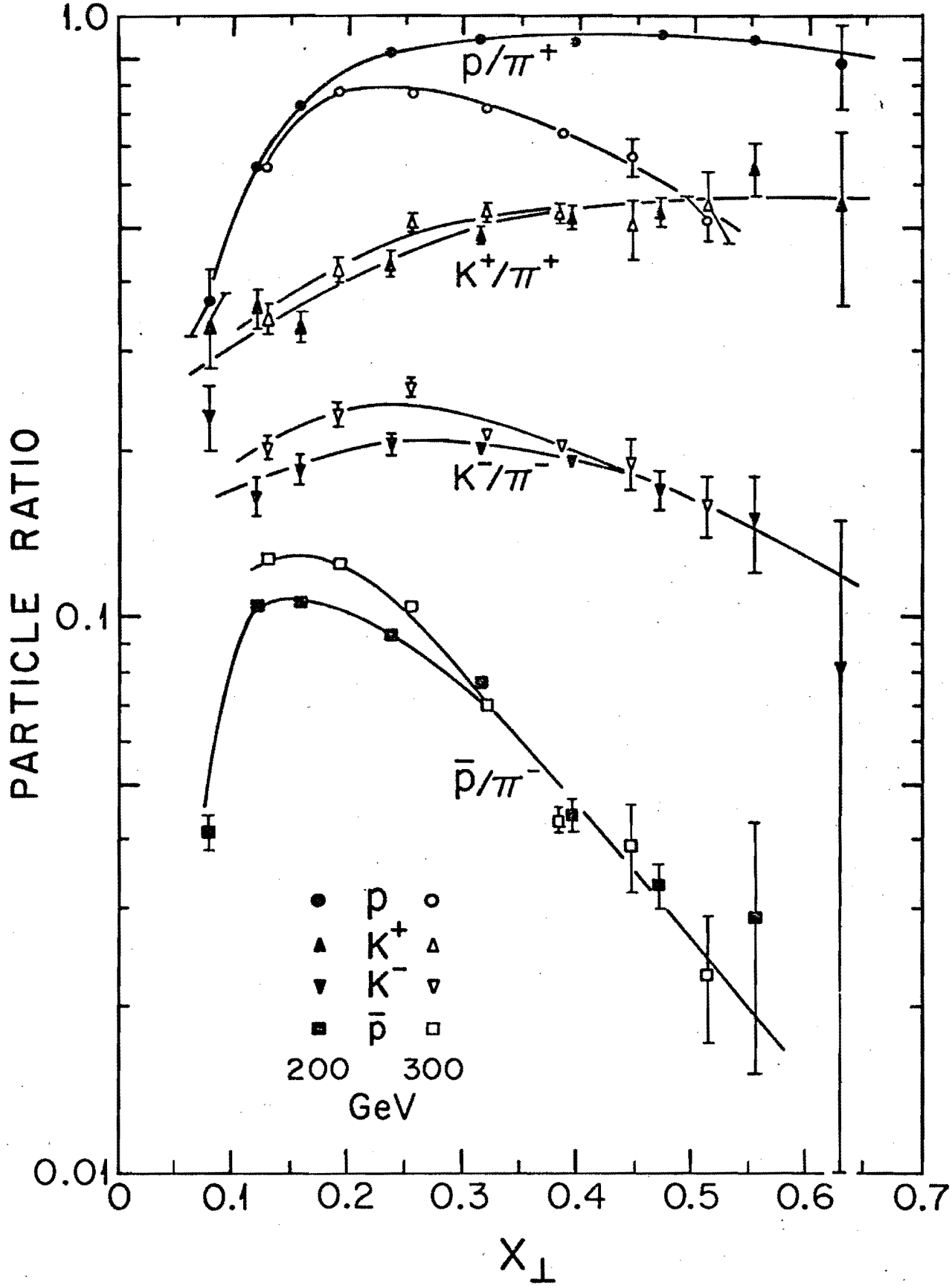
1.0
0.1
0.01
PARTICLE RATIO
p/π+
K+/π+
K−/π−
p̄/π−
p
K+
K−
p̄
200
300
GeV
0
0.1
0.2
0.3
0.4
0.5
0.6
0.7
X⊥

Figure 4

$p_\perp$ (GeV/c)	200 GEV $Ed\sigma(\pi)/d^3p$	200 GEV K/π	200 GEV p/π	300 GEV $Ed\sigma(\pi)/d^3p$	300 GEV K/π	300 GEV p/π
0.76	(2.69 ± 0.13) (2.08 ± 0.10) $\times 10^{-27}$	0.33 ± 0.05 0.23 ± 0.03	0.37 ± 0.05 0.041 ± 0.003	(2.89 ± 0.14) (2.55 ± 0.13) $\times 10^{-27}$		
1.14	(3.96 ± 0.20) (3.21 ± 0.16) $\times 10^{-28}$	0.358 ± 0.029 0.165 ± 0.013	0.646 ± 0.007 0.104 ± 0.002	(4.14 ± 0.21) (4.12 ± 0.20) $\times 10^{-28}$		
1.53	(6.04 ± 0.30) (5.31 ± 0.27) $\times 10^{-29}$	0.331 ± 0.020 0.186 ± 0.011	0.824 ± 0.009 0.106 ± 0.002	(6.26 ± 0.31) (7.07 ± 0.35) $\times 10^{-29}$	0.343 ± 0.021 0.201 ± 0.012	0.647 ± 0.007 0.127 ± 0.002
2.29	(2.56 ± 0.13) (2.03 ± 0.10) $\times 10^{-30}$	0.434 ± 0.021 0.204 ± 0.010	1.020 ± 0.011 0.093 ± 0.003	(2.95 ± 0.15) (2.97 ± 0.15) $\times 10^{-30}$	0.421 ± 0.018 0.231 ± 0.010	0.871 ± 0.009 0.124 ± 0.002
3.05	(1.25 ± 0.06) (0.98 ± 0.05) $\times 10^{-31}$	0.485 ± 0.015 0.201 ± 0.006	1.093 ± 0.011 0.076 ± 0.001	(1.77 ± 0.09) (1.59 ± 0.08) $\times 10^{-31}$	0.514 ± 0.015 0.260 ± 0.008	0.871 ± 0.004 0.104 ± 0.001
3.81	(6.77 ± 0.34) (5.01 ± 0.25) $\times 10^{-33}$	0.522 ± 0.024 0.191 ± 0.007	1.07 ± 0.02 0.044 ± 0.003	(1.35 ± 0.07) (1.14 ± 0.06) $\times 10^{-32}$	0.532 ± 0.020 0.214 ± 0.008	0.816 ± 0.013 0.069 ± 0.003
4.58	(3.86 ± 0.19) (2.85 ± 0.14) $\times 10^{-34}$	0.536 ± 0.033 0.170 ± 0.014	1.11 ± 0.03 0.033 ± 0.003	(8.78 ± 0.42) (8.46 ± 0.46) $\times 10^{-34}$	0.531 ± 0.022 0.205 ± 0.008	0.742 ± 0.015 0.043 ± 0.002
5.34	(2.38 ± 0.12) (1.65 ± 0.08) $\times 10^{-35}$	0.64 ± 0.07 0.15 ± 0.03	1.09 ± 0.07 0.029 ± 0.014	(9.45 ± 0.57) (6.99 ± 0.34) $\times 10^{-35}$	0.50 ± 0.06 0.19 ± 0.02	0.67 ± 0.05 0.039 ± 0.007
6.10	(1.30 ± 0.19) (1.06 ± 0.12) $\times 10^{-36}$	0.55 ± 0.19 0.08 ± 0.07	0.98 ± 0.17 < 0.01	(9.82 ± 0.61) (7.42 ± 0.53) $\times 10^{-36}$	0.55 ± 0.08 0.16 ± 0.02	0.52 ± 0.05 0.023 ± 0.006
6.87	(6.6 ± 1.7) (5.2 ± 1.6) $\times 10^{-38}$					
7.25	$(\quad)$ (1.6 ± 0.9) $\times 10^{-38}$					
7.63				(6.9 ± 2.0) (8.1 ± 2.1) $\times 10^{-38}$		

Table I

ADDENDUM TO NAL PROPOSAL 258

J. P. Boymond, P. A. Piroue*, and R. L. Sumner
Department of Physics, Joseph Henry Laboratories
Princeton University, Princeton, New Jersey 08540

and

J. W. Cronin, H. J. Frisch, and M. J. Shochet
The Enrico Fermi Institute
University of Chicago, Chicago, Illinois 60637

May 29, 1974

*Correspondent

We propose the construction of a muon detector on the other side of the incident π beam from the focusing spectrometer. Such a muon detector would permit a very sensitive search for the process $\pi^- + \text{nucleon} \rightarrow \mu^+\mu^- + X$ in addition to the proposed measurement of hadron and muon production at high $P_\perp$.

The rate for the reaction $\pi^- p \rightarrow \mu^+\mu^- + X$ is predicted [1,2,3] to be enhanced over that in proton-proton collisions by the parton model. This is due to the fact that a π^- has a "fast" anti-quark component, thereby facilitating the quark-antiquark annihilation into a high mass virtual photon, which then decays to a muon pair. Parton model predictions[2] for the invariant cross sections for single muons from proton-proton and π^- proton collisions are shown in Figure 1; one sees that at 300 GeV single muon production from pions is at least 10 times more copious than that from protons at $P_\perp = 3$ GeV/c.

The spectrum of single directly produced muons has already been measured in proton-proton collisions[4]; attachment A to this addendum is a report on our results from such a measurement performed in NAL Experiment 100. The results of this measurement are shown in Figure 3 of the attachment. The measured muon spectrum has the same shape as the pion spectrum, but is suppressed by a factor of $\sim 10^{-4}$. Figure 3 also shows the parton model[2] prediction for the single muon spectrum: one sees that even down to very small cross sections it is completely buried beneath the measured spectrum. Consequently, tests of the parton model predictions in p-p collisions must rely on the detection of muon pairs.

Figure 1 shows the situation for pion induced single muons -- one sees that if the production of muons by pions is the same as that measured with protons, it will be equal to the parton model predictions at $P_\perp \approx 4$ GeV/c, and at an invariant cross section $Ed\sigma/d^3p = 3 \times 10^{-37}$ cm^2 GeV^{-2}. This cross section is measurable with a π^- beam of 10^{10}/pulse at NAL. If the directly produced single muons measured at NAL are produced in low invariant mass pairs, such as the ρ, ω,ϕ, etc., then the requirement of detecting the second muon should provide the required discrimination to separate these events from those coming from high invariant mass pairs.

A possible layout for the spectrometer and the muon arm is shown in Figure 2. The central angle would be 100 mr, 90° in the c.m. for a 200 GeV/c incident beam. The muon arm subtends between 35 and 160 mr in the lab, and has an acceptance of 50 mr in azimuth. Three banks of scintillator hodoscopes separated by absorber determine the muon direction and identification.

Because of the requirement of transverse momentum balance, if the muon pair is assumed to have zero initial transverse momentum, the determination of the angle of the second muon is enough to determine its momentum. The invariant mass of the pair is already determined by the transverse momentum.

Figure 3 shows the rates for single muons and muon pairs in events/shift vs. $P_\perp$ measured in the spectrometer arm, as computed from the parton model calculation of G. Farrar[2]. At a $P_\perp$ of 3 GeV (invariant mass = 6 GeV/c^2), and with a 200 GeV beam of 10^{10} pions/pulse, one detects 8 events/shift. The one event/shift level is reached at a $P_\perp$ of 5 GeV/c.

In addition to adding the muon arm, we also have made some simple modifications to the NAL 100 spectrometer design that have increased its

solid angle by a factor of 2 to 32 μster and its momentum bite to ± 10%. This results in an increase of a factor of 4 in rate over the proposal values. The modifications consist of shortening the spectrometer so that the maximum measurable $P_\perp$ is 10 GeV/c, and replacing the main ring quadrupoles and bend magnets currently in use with 4Q 120 beam transport quadrupoles and 6-3-120 bend magnets, respectively. The new magnets have the added advantage that they run at much more reasonable currents than the present ones.

REFERENCES

1. R. P. Feynman, Photon Hadron Interactions, Benjamin, p. 163 (1972).
2. G. Farrar, CALTECH preprint CALT-68-422.
3. M. Einhorn and R. Savit, NAL preprint, NAL PUB-74/35-THY.
4. J. P. Boymond et al., see attached preprint (to be published). Also similar results have been presented at the Washington meeting by NAL experiments 70 and 184.

FIGURE CAPTIONS

Figure 1. Predictions of Farrar[2] for single muon production in pp (dotted curves) and π^- p collisions. The triangles represent 10^{-4} times the single pion production in proton-W collisions - this is a likely background of prompt muons.

Figure 2. A possible layout for the charged particle spectrometer and the muon arm.

Figure 3. Rates in events/shift for single muons and muon pairs for the apparatus described, as predicted by the model of Farrar.[2]

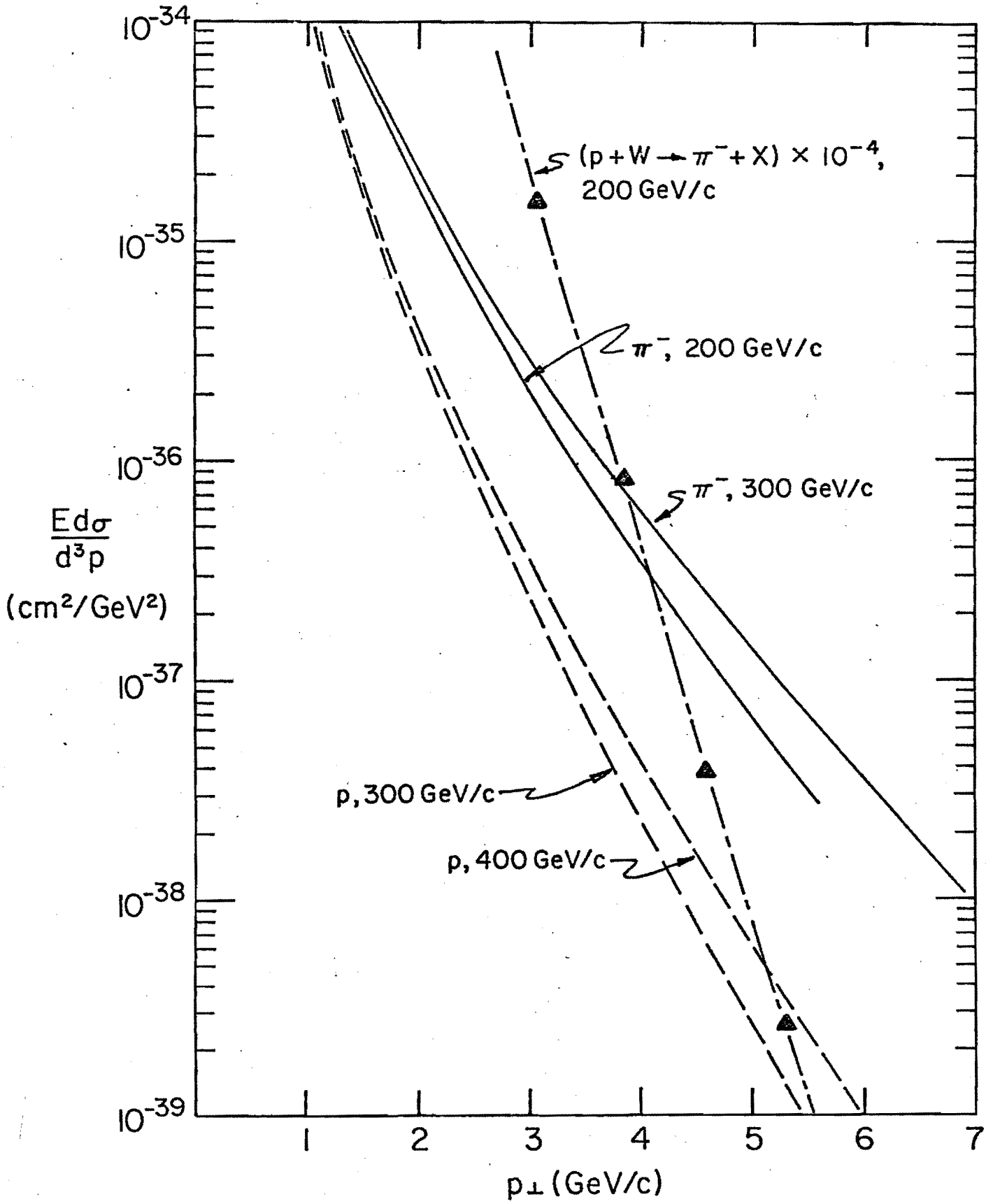
10^{-34}
10^{-35}
10^{-36}
10^{-37}
10^{-38}
10^{-39}
$\frac{E d\sigma}{d^3p}$
(cm^2/GeV^2)
$(p + W \rightarrow \pi^- + X) \times 10^{-4}$, 200 GeV/c
π^-, 200 GeV/c
π^-, 300 GeV/c
p, 300 GeV/c
p, 400 GeV/c
1
2
3
4
5
6
7
$p_\perp$ (GeV/c)

Figure 1

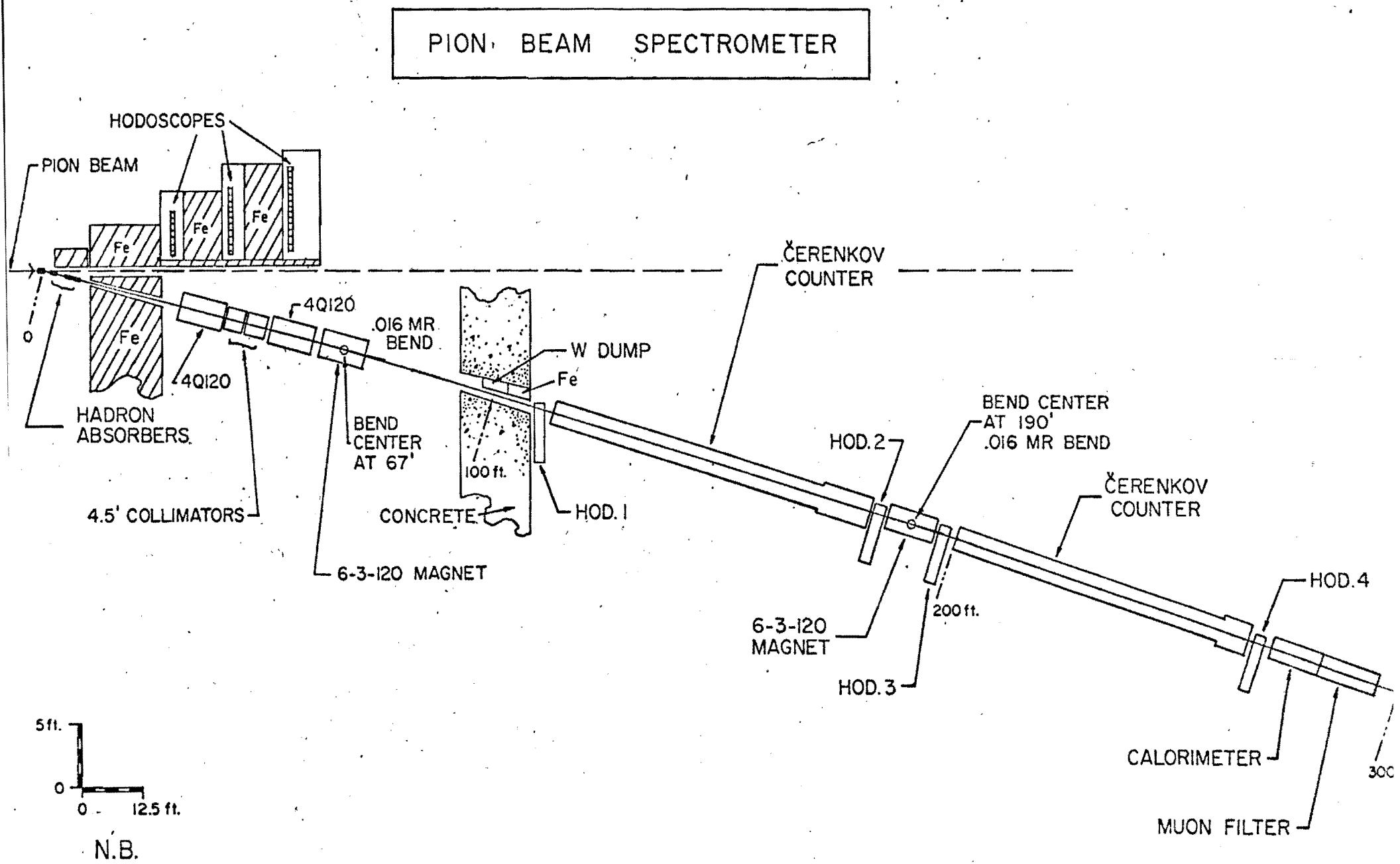
PION BEAM SPECTROMETER
HODOSCOPES
PION BEAM
Fe
Fe
Fe
Fe
0
HADRON ABSORBERS
4.5' COLLIMATORS
4Q120
4Q120
.016 MR BEND
BEND CENTER AT 67'
6-3-120 MAGNET
CONCRETE
100 ft.
W DUMP
Fe
HOD. 1
ČERENKOV COUNTER
HOD. 2
BEND CENTER AT 190' .016 MR BEND
6-3-120 MAGNET
HOD. 3
200 ft.
ČERENKOV COUNTER
HOD. 4
CALORIMETER
MUON FILTER
300
5 ft.
0
0 - 12.5 ft.
N.B.

Figure 2

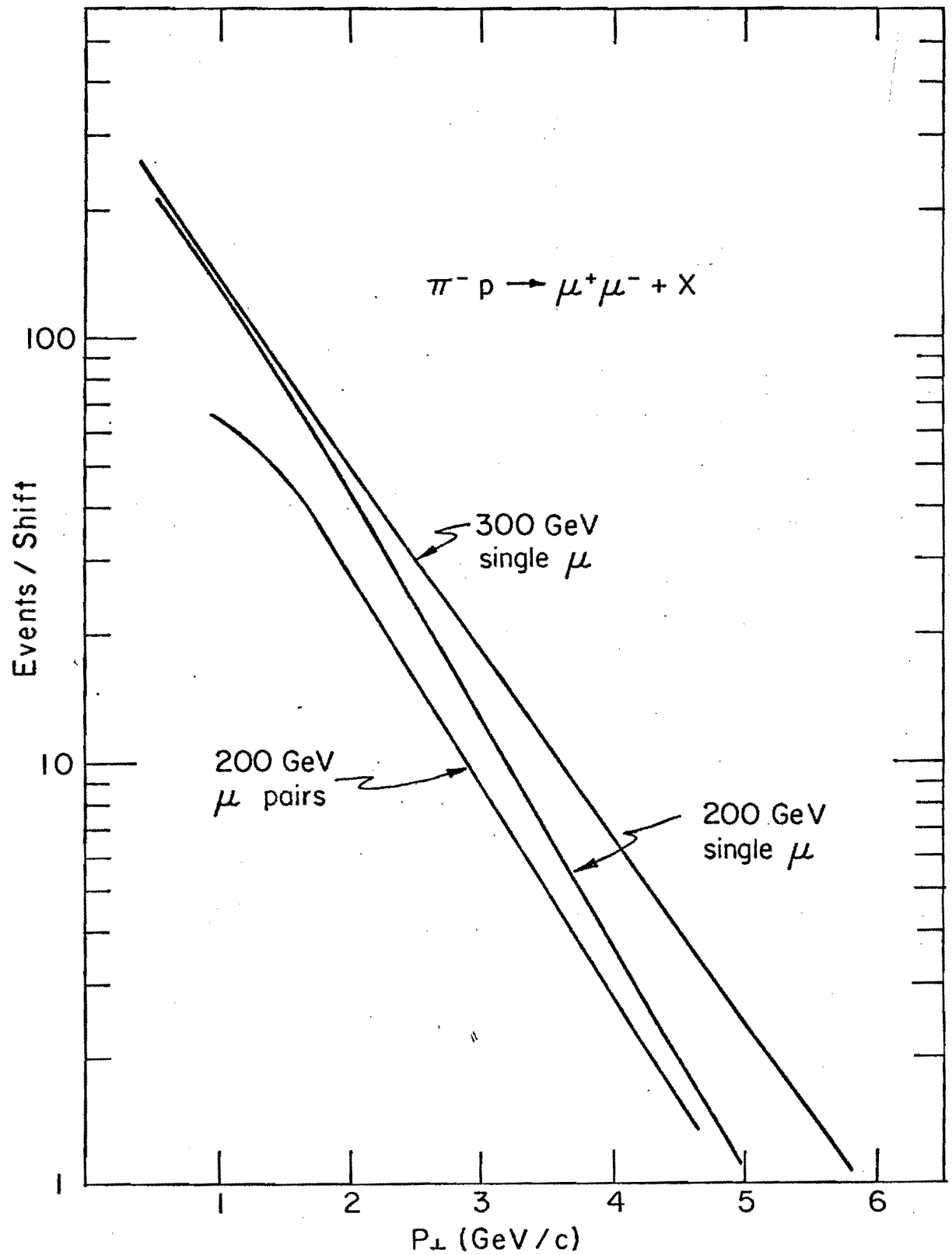
$\pi^- p \rightarrow \mu^+\mu^- + X$
100
10
1
Events / Shift
300 GeV
single μ
200 GeV
μ pairs
200 GeV
single μ
1
2
3
4
5
6
$P_\perp$ (GeV / c)

Figure 3

EFI-74-24

Observation of Large Transverse Momentum Muons Directly Produced by 300 GeV Protons*

J. P. Boymond, R. Mermod,† P. A. Piroué, and R. L. Sumner
Department of Physics, Joseph Henry Laboratories
Princeton University, Princeton, New Jersey 08540
and
J. W. Cronin, H. J. Frisch, and M. J. Shochet
The Enrico Fermi Institute
University of Chicago, Chicago, Illinois 60637

ABSTRACT

We have observed muons produced directly in Cu and W targets by 300 GeV incident protons. We find a yield of muons which is approximately a constant fraction (0.8×10^{-4}) of the pion yield for both positive and negative charge and for transverse momenta between 1.5 and 5.4 GeV/c.

In this letter we report on the observation of muons produced directly in nuclear targets by 300 GeV incident protons. Study of muon production at high transverse momentum was originally motivated by the search for the intermediate vector boson. Early experiments were carried out at the Argonne Z.G.S.[1] and the Brookhaven A.G.S.[2] with negative results. More recently, several experiments have shown evidence either for the direct production of single muons,[3,4] or muon pairs[5] in nucleon-nucleon collisions. Extensive theoretical work[6,7] suggests

that collisions of point-like constituents of the nucleon would result in the direct production of muons.

In this experiment, performed at the National Accelerator Laboratory (NAL), we have used an apparatus described in a previous publication.[8] It consists of a single arm focusing spectrometer equipped with two Cerenkov counters and a calorimeter to identify hadrons, and a 15-ft.-long steel filter sampled each 2.5 ft. with dE/dx counters to identify muons. The spectrometer viewed secondaries produced in a heavy target at an angle of 77 mrad relative to the incident 300-GeV proton beam. This angle corresponds to $\sim 90°$ in the nucleon-nucleon c.m. Direct muons from the target were separated from muons coming from π and K decays in flight with the aid of two absorbers which could be inserted into the spectrometer close to the target. The first absorber was a 23-in.-long W block with its upstream face 9.5 in. from the center of the target. The second absorber was a 42-in.-long Fe block with its upstream face 42 in. from the target. We used a 2-in.-long W target, primarily in runs with negative muons, and a 3-in.-long Cu target primarily in runs with positive muons.

Data were taken under three conditions: 1) no absorber, 2) W absorber inserted only, and 3) Fe absorber inserted only. Runs were made at 10 GeV/c intervals between 20 GeV/c and 70 GeV/c corresponding to transverse momenta ($P_\perp$) from 1.5 to 5.4 GeV/c. At 20 and 30 GeV/c, data were also taken with both absorbers in the beam as a consistency check. To verify that the muons were associated with the target, we also took data with the target removed for the three principal conditions at 20, 30 and 40 GeV/c.

For each absorber condition we measured the ratio of muons detected at the end of our apparatus to pions of the same charge detected by the apparatus

when the absorber was absent. Two counter telescopes which looked at the target at 90° laboratory angle permitted normalization of different runs. The yield of pions with no absorber was corrected for nuclear absorption in the remainder of the apparatus and for decay in flight.

The hadrons were attenuated by factors of $\sim$ 200 and $\sim$ 270 with the W and Fe absorbers respectively. These rather small attenuations resulted in a significant hadron penetration. These hadrons were identified by the combination of the Cerenkov counters and the hadron calorimeter. Those decaying appeared as muons. Thus the observed muons with absorber in place consisted of three components: 1) muons produced directly in the target, 2) muons produced by hadrons decaying upstream of the absorber, and 3) decay muons from hadrons which penetrated the absorber.

For process (3) the ratio of muons to pions[9] was directly measured at each momentum and polarity in runs without the absorbers; the corresponding muon yield in the absorber runs is calculated from the observed penetrating pions. The remaining muon yield coming from processes (1) and (2) is then corrected for the loss due to the absorber insertion (e.g. multiple scattering). Finally, the direct muon yield is obtained by linear extrapolation to zero decay path.

In Table I we present the reduction of the raw data from a typical run at 40 GeV/c. The absorber loss factors, calculated by Monte Carlo techniques, are presented in Table II. These factors account for the multiple scattering loss, as well as the increased yield due to acceptance of smaller $P_\perp$ when the absorber is in place. The dependence of yield on $P_\perp$ was taken from our previous measurements of hadron production.[8] We thus assume that the direct muon component has a similar dependence on $P_\perp$, an assumption that can be checked à postiori.

Figure 1 shows the corrected results of a typical run along with the predicted slope. The points are plotted at a distance $(d + \lambda)$ where d is the distance between the target and the upstream end of the absorber, and λ is the measured interaction length in the absorber.

The predicted slope can be obtained from the rate of hadron decay between the target and the absorber. It was calculated by numerical integration as a function of momentum. The yield of decay muons between the target and absorber depends on both K and π decays. Kaons are twice as effective as pions in producing detected muons. Thus the slope is sensitive to the K/π ratio at the target. Figure 2 shows for both charges the predicted and observed slopes plotted against the inverse of the muon momentum.

The agreement between calculated and observed slopes is a significant verification of the corrections which are quite different in nature for the two absorbers. The W absorber is more sensitive to the broadening of the acceptance because of its proximity to the target, but is less sensitive to multiple scattering for the same reason. The inverse is true for the Fe absorber.

Table III gives the ratio of direct muons to pions at the target for all conditions. The most striking aspect of these results is the constancy of the ratio μ/π. The constancy for different target materials is particularly interesting. In a separate experiment, to be reported in a subsequent publication, we have found the yield of pions per interacting proton at 3 GeV/c $P_\perp$ to be 3.5 times larger from a W target than a Be target. This effect is believed to be due to secondary scattering in the nucleus. Since the direct muons follow the same pattern, a strongly interacting, short lifetime source is suggested for the muons.

One such source can be the known vector mesons. For example, if ρ and ϕ were each produced with the same cross section as π, we would expect a ratio $(\mu/\pi) \times 10^4$ of 0.68, 0.46, and 0.33 at $P_\perp$ of 1.5, 3.0, and 4.5 GeV/c respectively.

In Figure 3 we plot the invariant cross section per nucleon for inclusive muon production. Also plotted is the inclusive pion cross section $\times 10^{-4}$ and the inclusive muon cross section expected from a model based on parton-antiparton annihilation.[10] It is clear that the yield of muons is everywhere in excess of the parton model prediction.

We wish to thank the staff of the Proton Section of NAL for their magnificent support of this experiment. We also wish to thank V. L. Fitch, S. B. Treiman, E. A. Paschos, and G. R. Farrar for valuable discussions. Finally, one of us (R.M.) wishes to thank NAL for its hospitality and support.

REFERENCES

*Work supported by the National Science Foundation and the U. S. Atomic Energy Commission.

†On leave at NAL from the University of Geneva.

1. R. C. Lamb et al., Phys. Rev. Letters 15, 800 (1965).
2. R. Burns et al., Phys. Rev. Letters 15, 830 (1965).
3. P. J. Wanderer et al., Phys. Rev. Letters 23, 729 (1969).
4. Bondarenko et al., (Paper 927), Proceedings of the XVI International Conference on High Energy Physics, Vol. 2, p. 329, (1972), edited by J. D. Jackson and A. Roberts.
5. J. Christenson et al., Phys. Rev. Letters 25, 1523 (1970).
6. S. D. Drell and T. M. Yan, Phys. Rev. Letters 25, 316 (1970).
7. J. D. Bjorken, Proceedings of II International Conference on Elementary Particles, Aix-en-Provence (1973), Journal de Physique, 34, C1-385, (1973).
8. J. W. Cronin et al., Phys, Rev. Letters 31, 1426 (1973).
9. For convenience we normalize to pions; the pions serve as a measure of all hadrons.
10. G. R. Farrar, California Institute of Technology preprint, CALT - 68 - 422, (1974); also private communication.

FIGURE CAPTIONS

Figure 1. Plot of data reduced in Table I. The dashed curve shows the linear extrapolation to the target. The solid line is the calculated slope.

Figure 2. Plot of observed slope and calculated slope vs. reciprocal of the muon momentum. The points are the experimentally measured slopes; the solid line is the calculated slope.

Figure 3. Plot of the invariant cross section for direct muon production vs. $P_{\perp}$. Also shown is the pion cross section x 10^{-4} and the cross section predicted by a parton model

TABLE CAPTIONS

Table I. Reduction of raw data to direct muon yield at the target. Processes (1), (2), and (3) are referred to in the text. Tungsten and Iron refer to the particular absorber used.

Table II. Calculated absorber loss factors.

Table III. Ratio of directly produced muons to pions in the proton-nucleus collision. The observed pions emerging from the 0.4-interaction-length target are multiplied by a factor 1.25 to account for absorption in the target itself.

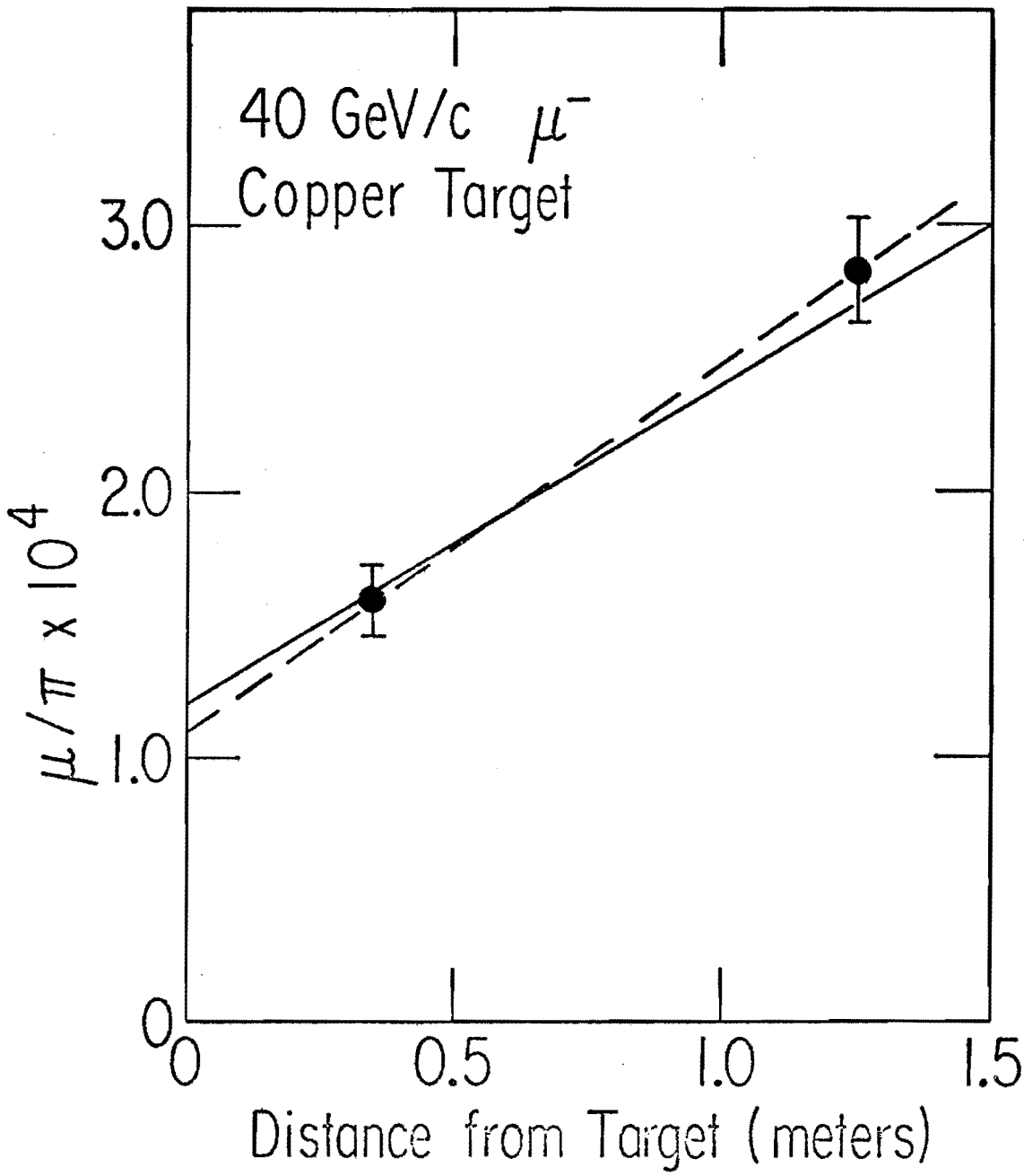
40 GeV/c μ^-
Copper Target
3.0
2.0
1.0
0
$\mu/\pi \times 10^4$
0
0.5
1.0
1.5
Distance from Target (meters)

Figure 1

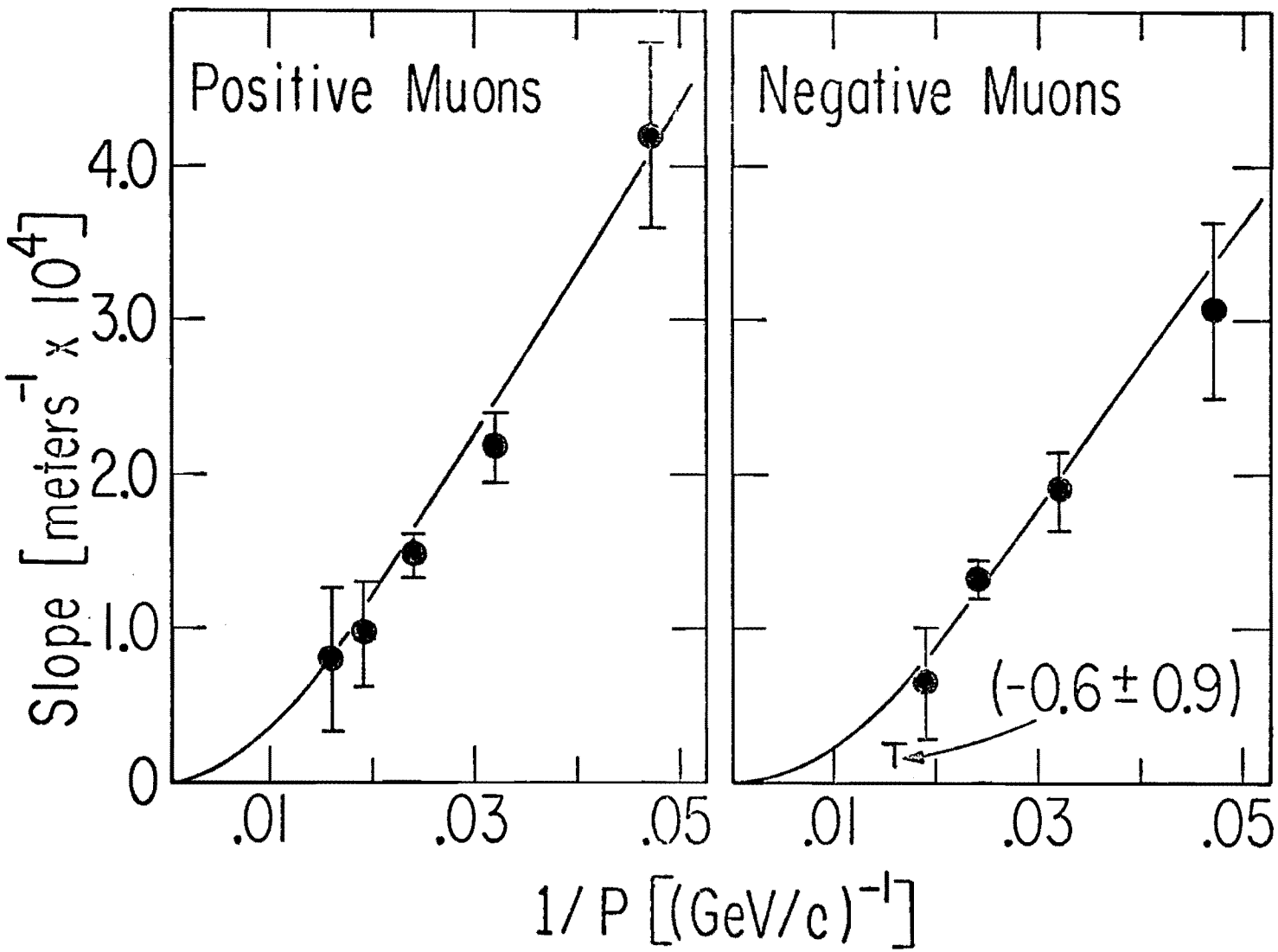
Positive Muons
Negative Muons
Slope [meters^{-1} x 10^4]
4.0
3.0
2.0
1.0
0
.01
.03
.05
(-0.6 ± 0.9)
1/ P [(GeV/c)$^{-1}$]

Figure 2

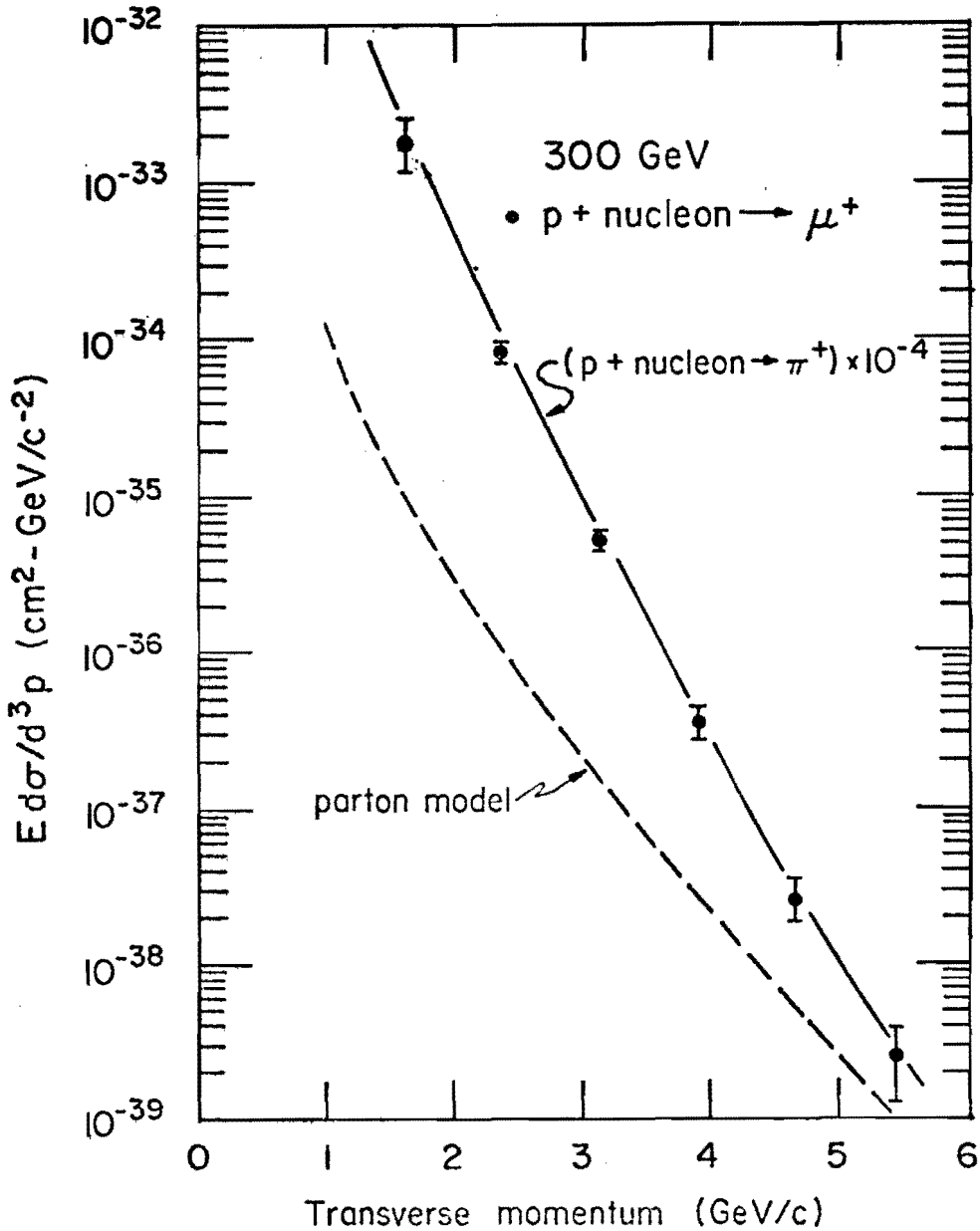
300 GeV
• p + nucleon → μ+
(p + nucleon → π+) × 10-4
parton model
E dσ/d3p (cm2 - GeV/c-2)
Transverse momentum (GeV/c)
10-32
10-33
10-34
10-35
10-36
10-37
10-38
10-39
0
1
2
3
4
5
6

Figure 3

	Tungsten	Iron
Observed muons	795±28	623±25
Observed pions	13580	4985
Ratio μ/π without absorber	$(2.03\pm0.10) \times 10^{-2}$	
Muons from hadron penetration of absorber (process (3))	276±13	101±5
Muons from processes (1) and (2)	519±31	522±26
Absorber loss factor	0.71±0.04	0.40±0.02
Corrected muons from processes (1) and (2)	731±60	1305±92
Pions at target	4.60×10^{6}	4.62×10^{6}
Muons/Pions at target	$(1.59\pm0.13) \times 10^{-4}$	$(2.83\pm.20) \times 10^{-4}$
Effective distance to target (meters)	0.35	1.25
Extrapolated μ/π at target	$(1.10\pm0.15) \times 10^{-4}$	

Table I

Momentum (GeV/c)	Tungsten	Iron
20	0.42±0.03	0.182±0.015
30	0.56±0.03	0.300±0.015
40	0.71±0.04	0.40±0.02
50	0.81±0.05	0.47±0.02
60	0.87±0.04	0.54±0.02
70	1.02±0.04	0.62±0.03

Table II

$P_\perp$ (GeV/c)	$\mu/\pi \times 10^4$ (Target) Positive	Negative
1.62	.66±.25 (Cu)	.86±.20 (W)
2.38	.72±.11 (Cu)	.67±.12 (W)
3.15	.88±.18 (Be)	- - -
3.15	.94±.16 (Cu)	.88±.12 (Cu)
3.15	.60±.15 (W)	.74±.16 (W)
3.91	.98±.23 (Cu)	.88±.26 (W)
4.67	.87±.30 (Cu)	1.02±.34 (W)
5.44	.94±.47 (Cu)	1.20±.46 (W)

Table III